Engineered Science
DOI: https://dx.doi.org/10.30919/es1170

New Insights into the Early-Age Time-Dependent Dielectric Evolution of Pozzolan-Modified Eco-Efficient Cement Pastes Within a Frequency Range of 200 Mhz To 6500 Mhz: Experiments and Statistical Modeling

Natt Makul[1] and Gritsada Sua-iam[2,*]

Abstract

Exploring the dielectric properties of pozzolan-modified eco-efficient cement pastes has become an essential field of research in the quest for innovative construction materials. This study investigates the intricate relationship between dielectric constant (ε') and loss tangent ($tan\ \delta$) in various cement paste compositions, providing significant insights into their electronic characteristics. Through a comprehensive analysis, we examine the effects of both the type and dosage of pozzolan on these properties, shedding light on how these parameters affect the overall performance of the materials. The results of our analysis reveal intriguing patterns. Particularly noteworthy is the scenario where 30 wt% of cement is replaced with diatomite, resulting in a significant decrease in the loss tangent from 1.06676×10^{-9} to 4.76856×10^{-11}. This finding underscores the potential of diatomite as a viable modification to enhance the energy dissipation properties of cementitious materials. These observations have significant implications for developing durable and resilient structures and the sustainable integration of industrial waste into construction materials. This study emphasizes the importance of understanding the dielectric behavior exhibited by cement paste blends. By examining the correlation between different types of pozzolan, their respective dosages, and the resulting variations in dielectric characteristics, this research makes a valuable contribution to the extensive materials science and engineering field.

Keywords: Eco-efficient cement; Pozzolans; Dielectric constant; Loss tangent; Frequency; Statistical modeling.
Received: 03 January 2024; Revised: 05 April 2024; Accepted: 05 April 2024.
Article type: Research article.

1. Introduction

Concrete is the largest manufactured product by weight globally, serving a crucial function in the development of concrete-based goods when mixed with water and mineral components. After water, it stands as the second most frequently employed material worldwide. These elements make up a significant portion of the building sector.[1] In construction, cement-based materials have long played an indispensable role, forming the foundation upon which societies have erected their infrastructures and architectural marvels.[2] These materials derive their exceptional strength, durability, and versatility from the intricate interplay of chemical reactions and physical properties.[3,4] The process of Portland cement hydration, a complex blend of chemical and physical phenomena, critically shapes the microstructure and overall performance of cement-based materials.[5,6] Among the physical properties offering potential insight into the hydration process, the dielectric property stands out as promising for monitoring purposes.[7] As the convergence of science and engineering advances, so does our comprehension of cement-based materials, instigating a progressively deeper investigation into their characteristics and potential applications. Within this exploration, the dielectric properties of these materials have emerged as a captivating avenue of study, yielding profound insights into their internal dynamics and temporal evolution.[8–12] Numerous empirical studies have delved into the dielectric permittivity of cement-based

[1] *Department of Civil Engineering Technology, Faculty of Industrial Technology, Phranakhon Rajabhat University, 9 Changwattana Road, Bangkhen, Bangkok, 10220, Thailand.*
[2] *Department of Civil Engineering, Faculty of Engineering, Rajamangala University of Technology Phra Nakhon (RMUTP), 1381 Pracharat Sai 1 Road, Wong Sawang, Bang Sue, Bangkok 10800, Thailand.*
**Email:* gritsada.s@rmutp.ac.th (G. Sua-iam)

materials, spanning from cement paste and mortar to concrete at varying scales.[4,7,13–25]

Dielectric properties, characterized by permittivity and loss tangent parameters, govern how materials interact with electric fields.[17,26-29] Permittivity measures how easily a material can be polarized by an electric field, determining its ability to store electrical energy in an electric field. A higher permittivity allows the material to store more electric flux.[16–20,28,30-32] The loss tangent, also known as the dissipation factor, measures the energy lost as heat when an electric field is applied to a material. It is the ratio of the imaginary part of the permittivity to the real part of the permittivity. A high loss tangent indicates that the material dissipates a significant amount of energy as heat when exposed to an electric field.[17,18,27,28,32–34] In the context of cement-based materials, these properties are not merely academic curiosities; they hold the potential to provide real-time insights into the crucial process of hydration. A symphony of chemical reactions and transformations marks the journey from mixing to setting, where cement particles react with water to form a solid matrix.[10,14,15,35] This intricate dance dictates the material's ultimate strength, durability, and performance.[15,18,30,36,37] The dielectric response, a signature of this underlying molecular activity, offers a window into the intimate progression of these materials over time.[16,18,38]

Incorporating pozzolanic materials into cement-based formulations has emerged as a strategy to enhance both the sustainability and performance of these materials.[39] Pozzolanic materials contain silica or alumina and occur naturally in the earth's crust or are produced as by-products of various industrial processes.[40,41] When pozzolanic materials are added to cement, they undergo a chemical reaction with the portlandite formed during the cement hydration process, resulting in lower porosity and increased cement strength.[39,41,42] The use of pozzolanic materials in cement and concrete has significantly increased, primarily due to their manifold advantages. These benefits include reduced cement use, lower production costs, and enhanced durability of the concrete. Researchers are also exploring using pozzolanic waste materials, such as fly ash, calcium carbonate, diatomite, and silica fume, as alternative resources for cement. This alternative binder is significant as it can reduce the energy consumption and carbon dioxide emissions associated with ordinary Portland cement.[40,41,43,44] Beyond their direct influence on mechanical properties, these additives impact the dielectric behavior of the materials. The dynamic nature of dielectric properties and the evolving presence of pozzolanic components form the core of a captivating research avenue. However, within this panorama of effects, the influence of pozzolans on the dielectric properties of cement-based materials remains relatively unexplored, especially concerning their temporal evolution. Investigating the synergistic effects of these materials promises to enrich our understanding of material science and unlock practical applications.

Previous research has extensively explored the dielectric characteristics of cementitious materials, revealing a broad spectrum of potential applications. Hamadouche *et al*.[16] utilized simulations to gain insight into the behavior of C-S-H gel, while Liu *et al*.[19] investigated the dielectric properties of C_3S paste. Ley-Hernandez *et al*.[9] introduced a revised model for the kinetics of cement hydration. Tsonos *et al*.[4] examined the electrical properties of mortar throughout the hardening process, whereas Jumrut *et al*.[45] analyzed the dielectric behavior of geopolymer mortar. Shen *et al*.[7] developed nondestructive testing techniques for concrete, while Zhong *et al*.[46] evaluated concrete strength through dielectric testing. Dinh *et al*.[18] investigated concrete's dielectric response to frequency and moisture content. Malkawi *et al*.[37] observed the geopolymerization process in pozzolanic materials by analyzing dielectric properties, and Li *et al*.[47] explored the electromagnetic properties of cement paste combined with supplementary materials. These studies collectively emphasize the significance of dielectric characteristics in understanding and managing the behavior of cementitious materials. Beyond its traditional use in construction materials, using the dielectric constant to determine the water-to-cement ratio in plastic concrete could have significant engineering applications in non-destructive testing of concrete structures, moisture monitoring in building materials, and concrete production quality control.[48] Also, the development and application of cement-based anchoring materials have the potential for various industrial and engineering processes.[49]

It is within this gap that the current study takes root. By systematically investigating the effects of different types and dosages of pozzolans on the dielectric properties of hydraulic Portland cement pastes, this research aims to illuminate the underexplored facets of the electrodynamic behavior of cementitious systems. These investigations delve deep into the nuances of how the dielectric constant (ε') and loss tangent ($tan\ \delta$) evolve over time and across a spectrum of frequencies. In doing so, the study aspires to uncover the intricate interplay between pozzolanic materials and the electrodynamic realm of cement-based systems and offer a nuanced perspective on the potential of dielectric monitoring as a tool for studying cement hydration kinetics. Through meticulous experimentation and comprehensive analysis, this research endeavors to enrich the understanding of how pozzolanic materials, often hailed for their cement-enhancing qualities, influence the time-dependent dielectric properties of cementitious matrices. By traversing the continuum of time and frequency, the study seeks to interpret the resonances and harmonics embedded within the dielectric landscape of these materials. As the chapters unfold, the dielectric constant and loss tangent symphony interweave with the narrative of pozzolanic influence, casting new light on the enigmatic world of cement hydration and its broader implications for construction science.

2. Materials and methods

2.1 Materials

Cement and pozzolans have been chosen for analysis because of their important roles in the composition and improvement of cementitious materials. Cement acts as the main binder in concrete, while the other components are supplementary cementitious materials that enhance the properties of the cement mixture. To understand the time-dependent dielectric properties of materials, we carefully selected critical components to formulate eco-efficient cement pastes. Each element brings unique characteristics to the intricate interactions defining the material's behavior.

2.1.1 Eco-efficient cement

The foundation of these cementitious pastes lies in the eco-efficient cement obtained from a local company in Thailand that is compliant with ASTM C1157.[50] It boasts a composition characterized by a high content of calcium oxide (CaO), accompanied by significant proportions of silicon dioxide (SiO_2), aluminum oxide (Al_2O_3), and iron oxide (Fe_2O_3). Table 1 provides the chemical composition of eco-efficient cement, and Fig. 1 illustrates a ternary-plotted diagram. These elements collaborate to form a blend well-suited for hydration, contributing to the complex network of chemical reactions determining the material's mechanical strength and durability. Fig. 2 presents the grading curves of cement used in this study with a mean particle size of 10.3 µm and a specific surface area of 2311 m²/kg. X-ray powder diffraction (XRD) analysis confirms the presence of tricalcium silicate (C_3S) as the primary mineral phase, a crucial contributor in the early stages of cement hydration, along with the identification of calcite ($CaCO_3$) as an additional component.

2.1.2 Pozzolans

Pozzolans introduce a diverse array of materials with unique compositions and properties. Fly ash, sourced from an electrical power plant as per ASTM C618,[51] exhibits a significant content of silica (SiO_2), aluminum oxide (Al_2O_3), and iron oxide (Fe_2O_3) of more than 53%. This combination enhances the material's latent hydraulic properties, improving its ability to react with calcium hydroxide formed during cement hydration. Calcium carbonate, often derived from natural sources, contributes a substantial amount of calcium oxide (CaO), exceeding 96%. Its larger mean particle size of 34.9 µm and specific surface area of 1200 m²/kg position it as a potential influencer of paste workability and rheology. Diatomite, a mineral-rich material, is characterized by its high silica content (>78%) and the presence of aluminum oxide (Al_2O_3) and iron oxide (Fe_2O_3). The pozzolanic activity allows for developing extra calcium silicate hydrate in cement. The analysis of diatomite is driven by its distinctive composition, which can enhance the material's microstructural development and increase its mechanical properties. Furthermore, the porosity and insulative properties of the material contribute to the enhancement of dielectric properties in specific applications. Finally, condensed silica fume, a finely divided amorphous silica material in line with ASTM C1240,[52] stands out for its dominant silica content (> 90%). With its minute mean particle size of 323 µm and specific surface area of 75.82 m²/kg, it plays a significant role in paste packing density and surface reactivity. Table 1 provides the chemical composition of pozzolan materials. The grading curves and XRD patterns of pozzolans used in this study are presented in Figs. 2 and 3, respectively.

2.1.3 Chemical admixture

Per ASTM C494,[53] high-range superplasticizer for Type G admixture is introduced in liquid form with a specific gravity of 1.03. These superplasticizers contain polycarboxylate ether polymers and undergo special formulation to provide exceptionally high-water reduction, significantly improved slump retention, and enhanced microstructural development.

2.1.4 Water

The distilled water used in the paste mixes has a typical pH of 7.5. It lacks any impurities or additives that could affect the chemical reactions within the cementitious matrix.

2.2 Concept mix design and proportions

The essence of investigating the time-dependent dielectric properties of eco-efficient cement lies in the individual materials and their intricate combinations. We meticulously crafted eight distinct mix compositions, each a fusion of hydraulic Portland cement and specific pozzolanic components. These concoctions, each representing a unique blend of components, serve as the canvases upon which the dielectric properties are revealed, unveiling the dynamic interplay between materials and time.

Table 1. Chemical compositions of cement, pozzolan, and mineral admixtures (%m/m).

Materials	Na_2O	MgO	Al_2O_3	SiO_2	SO_3	K_2O	CaO	Fe_2O_3	LOI
Eco-efficient cement	0.26	0.92	**3.18**	**14.29**	2.16	0.43	**71.25**	3.19	1.86
Fly ash	1.96	2.58	**13.05**	**25.58**	5.42	2.02	**27.90**	14.43	2.32
Calcium carbonate	0.01	1.03	**0.66**	**1.36**	0.03	0.07	**96.36**	0.33	4.65
Diatomite	0.14	0.57	**13.74**	**78.88**	0.03	1.98	**0.63**	3.45	6.34
Silica fume	0.20	0.72	**0.15**	**91.69**	0.96	2.32	**0.44**	0.04	0.93

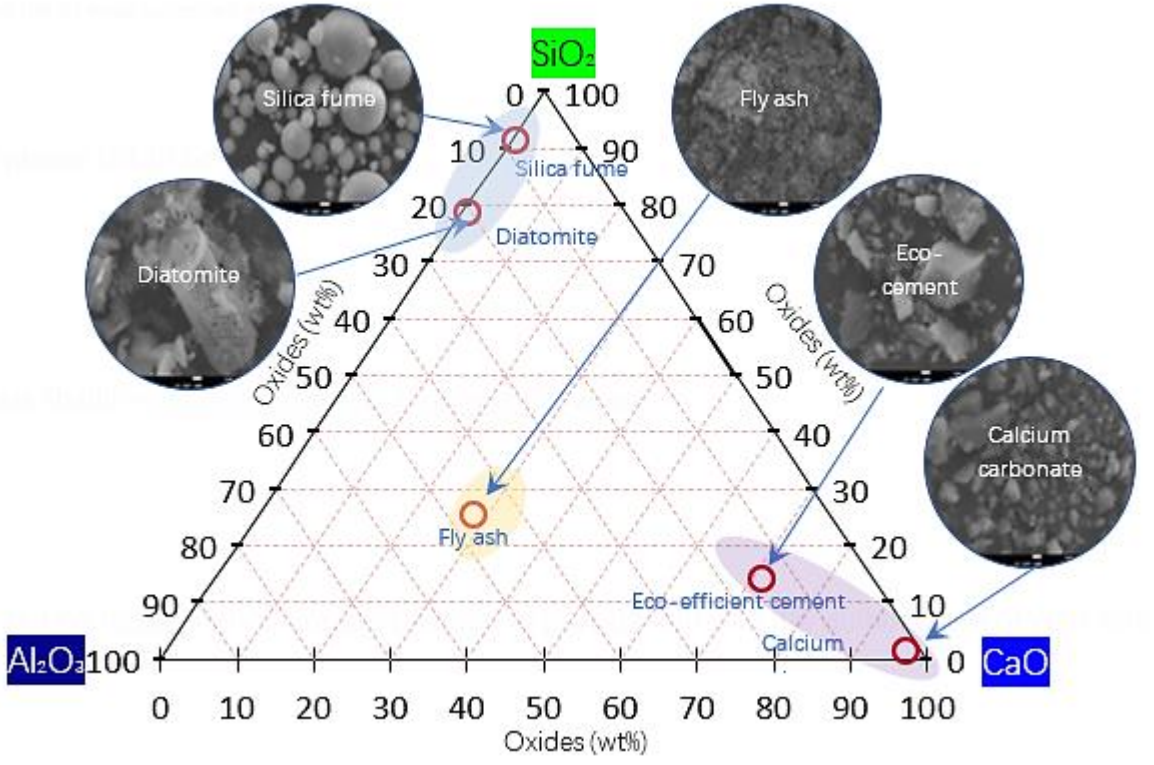

Fig. 1 Ternary-plotted diagram of eco-efficient cement, fly ash, calcium carbonate, diatomite, and silica fume.

The conceptually diverse mix designs offer a multifaceted exploration of the interplay between pozzolans and dielectric attributes by systematically varying pozzolan types and proportions. The different compositions of the pastes used in this investigation are presented in Table 2.

- **FA10 and FA30**: In this mix, 10 wt% and 30 wt% replacements of eco-efficient cement, respectively, are replaced with fly ash. The presence of fly ash and its pozzolanic characteristics could influence the material's early-age reactions, potentially affecting its dielectric properties.
- **CC10 and CC30**: By incorporating 10 wt% and 30 wt% of calcium carbonates, this mix investigates the influence of this alternative pozzolan on dielectric properties, reflecting the potential impacts of different mineralogical compositions.
- **DM10 and DM30**: This mix introduces diatomite at replacement levels of 10 wt% and 30 wt%, aiming to investigate the influence of this mineral-rich material on the dielectric properties of cementitious pastes.
- **SF8 and SF15**: With 8 wt% and 15 wt% silica fume replacement, this mix dissects the effect of this amorphous material on dielectric behavior, considering the influence of its unique properties.

Each mix composition adheres to a consistent water-to-powder ratio (w/p) of 0.45, ensuring uniform paste workability. All mixtures maintain an admixture dosage of 1.5% power materials. These controlled parameters lay the foundation for a systematic investigation into the impact of pozzolan type and dosage on the dielectric properties of eco-efficient cement pastes.

2.3 Sample preparation and testing

Studying time-dependent dielectric properties in eco-efficient cement requires meticulous sample preparation and testing protocols. The test program is designed to capture the material's evolving dielectric behavior from the initial mixing stage to a 360-minute (6-hour) timeframe.

Table 2. Compositions of the pozzolan-modified eco-efficient cement pastes used in this investigation (wt%).

Mix	Eco-efficient cement	Fly ash	Calcium carbonate	Diatomite	Silica fume	w/p	Admixture
FA10	90	10	-	-	-	0.45	1.5
FA30	70	30				0.45	1.5
CA10	90	-	10	-	-	0.45	1.5
CA30	70	-	30			0.45	1.5
DM10	90	-	-	10	-	0.45	1.5
DM30	70	-	-	30	-	0.45	1.5
SF8	92	-	-	-	8	0.45	1.5
SF15	85	-	-	-	15	0.45	1.5

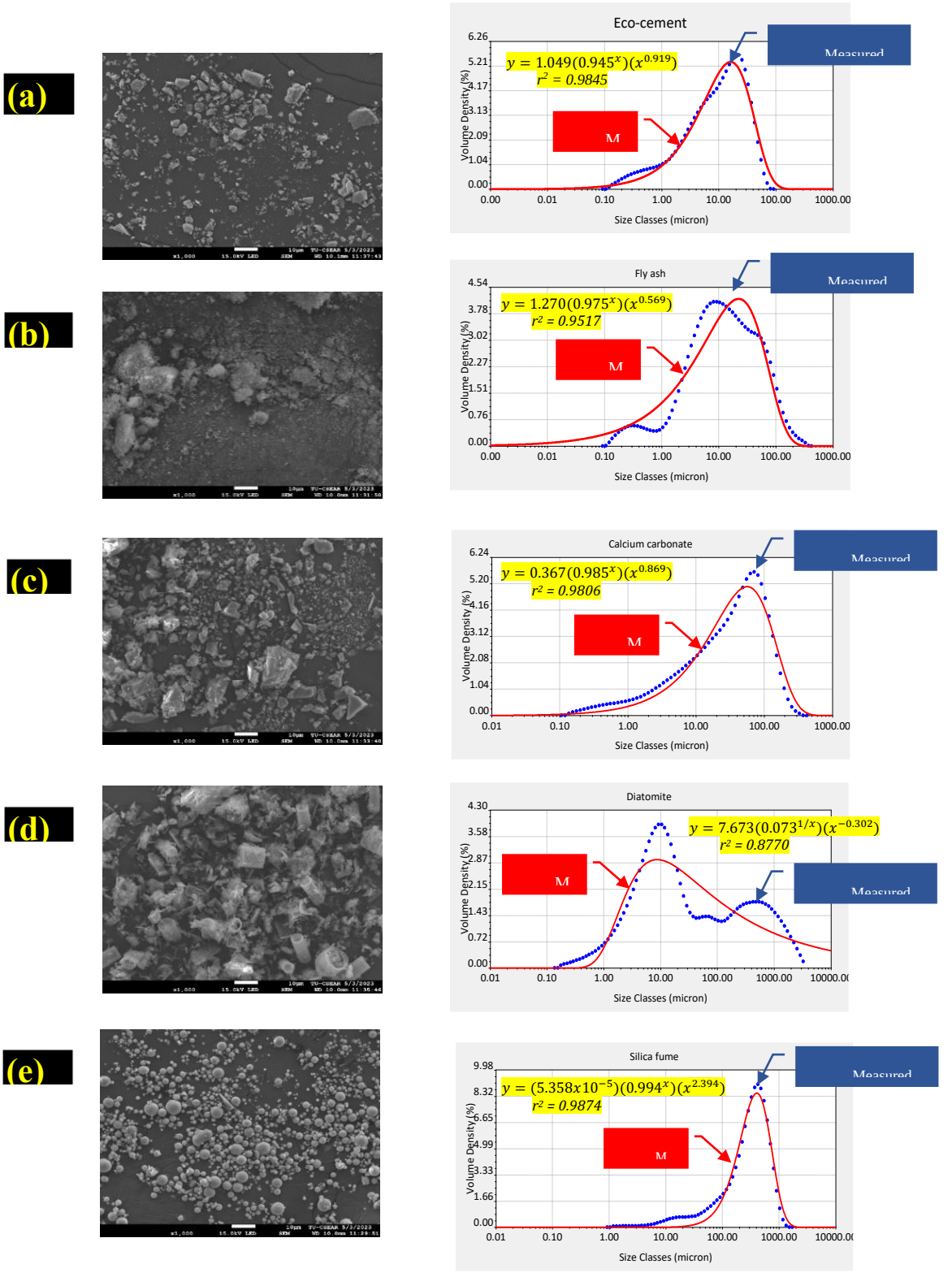

Fig. 2 The morphologies of (a) eco-efficient cement, (b) fly ash, (c) calcium carbonate, (d) diatomite, and (e) silica fume.

2.3.1 Sample preparation

To effectively investigate the dielectric properties of cementitious materials, it is crucial to carefully prepare samples, ensuring that each mixture is coherently composed of its various components. The process commences with the precise blending of hydraulic Portland cement and specific pozzolanic materials, with meticulous attention to the composition of each mixture. Eight distinct mix designs are involved, each requiring a precise choreography of steps. Cement and specific pozzolans are meticulously introduced and weighed to achieve the desired replacement levels. The dry ingredients are carefully mixed in a controlled environment to attain uniformity and eliminate potential variations. Subsequently, distilled water, as indicated in Fig. 4

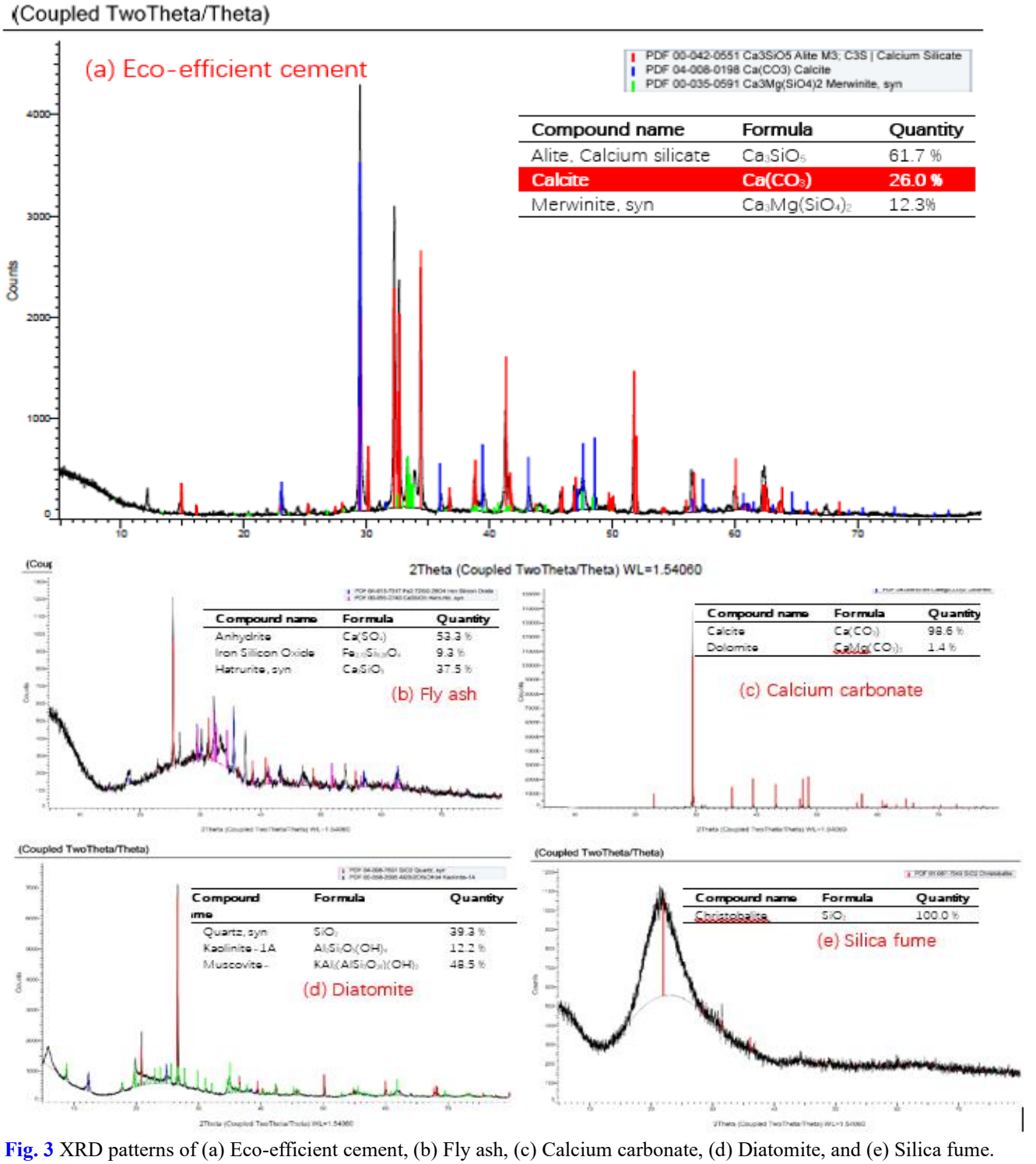

Fig. 3 XRD patterns of (a) Eco-efficient cement, (b) Fly ash, (c) Calcium carbonate, (d) Diatomite, and (e) Silica fume.

for dielectric constants (ε') and loss tangent ($tan\ \delta$), is introduced to the stage, maintaining a consistent water-to-powder ratio of 0.45. The equation (1) that represents the relationship between the loss tangent (tan δ) and the dielectric constant (ε') of a mixing water as a function of frequency (f) is given by

$$tan\ \delta\ (f, \varepsilon\wedge') = z0 + A_1\ f + A_2 f^2 + A_3 f^3 + A4 f^4 + A5 f^5 + B_1\varepsilon' + B_2\varepsilon'^2 + B_3\varepsilon\wedge'^3 + B_4\varepsilon\wedge'^4 + B_5\varepsilon\wedge'^5 \quad (1)$$

This equation is a polynomial equation that describes how ε' and tan δ change with frequency. The coefficients in the equation (A1, A2, A3, A4, A5, B1, B2, B3, B4, and B5) are calculated using optimization techniques to minimize the mean squared error between the fitted model and the experimental data (Table 3).

Hydration plays a pivotal role in the chemical reactions that facilitate the transformation of cement from a paste into a solid matrix, with water catalyzing this process. To further enhance a high-range superplasticizer, the admixture is added at a dosage of 1.5% of powder materials. This addition helps control the workability of the paste and ensures consistency

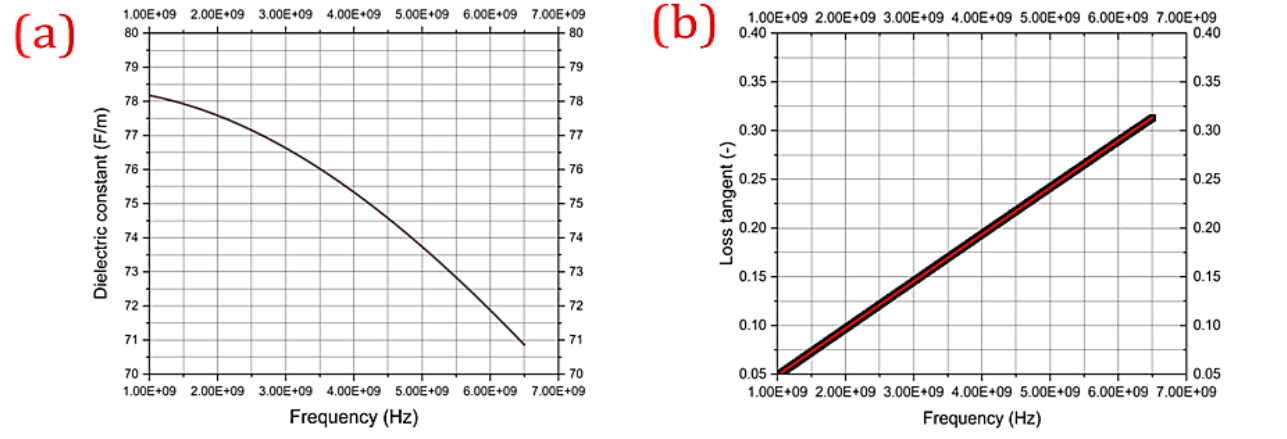

$$\varepsilon'(f) = \frac{a}{1+bf+cf^2},$$

a = 78.37836 ± 9.97042E-4
b = 1.25163E-13 ± 9.02357E-15
c = 2.49186E-21 ± 1.31591E-24
R^2 = 1.0000

$$tan\ \delta(f) = af^b,$$

a = 5.45185E-11 ± 2.39575E-13
b = 0.99456 ± -1.97362E-4
R^2 = 1.0000

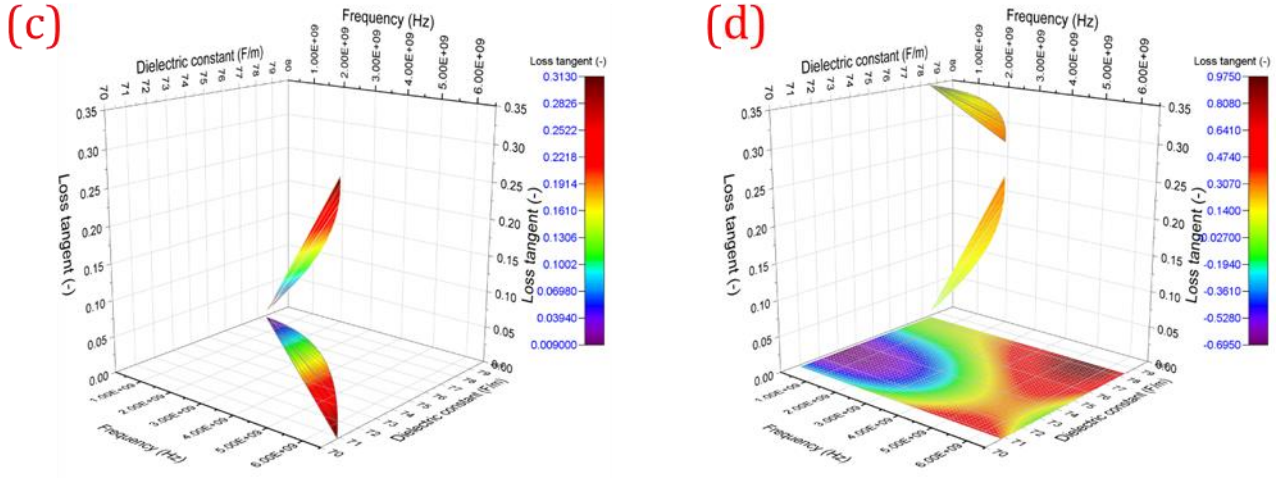

Measured value Model results

Fig. 4 The dielectric constant (ε') and loss tangent ($tan\ \delta$) of mixing water.

Table 3. The statistical model for predicting dielectric constant values of mixing water.

z0	**A_1**	**A_2**	**A_3**	**A_4**	**A_5**
182959.07032 ± 850.57268	7.60438E-11 ± 3.20719E-12	-4.84022E-20 ± 4.76108E-21	2.18658E-29 ± 2.26386E-30	2.99719E-40 ± 1.01439E-39	-3.76418E-49 ± 1.07846E-49
R^2	**B_1**	**B_2**	**B_3**	**B_4**	**B_5**
0.99991	-12261.33436 ± 31.8878	329.33425 ± 0.33171	-4.43126 ± 0.00523	0.02987 ± 6.92222E-5	-8.06455E-5 ± 2.6665E-7

across all samples. A mechanical mixer is used for thorough mixing of dry materials, ensuring uniformity before gradually adding water and admixtures to achieve a uniform mixture. The mixing process continues for a standard duration at a controlled room temperature of 25 ± 1 °C, typically lasting 3-5 minutes to ensure the production of a homogeneous paste or concrete mix. Immediately after mixing, the mixture is poured into molds, which are cylindrical with dimensions of 50 mm in height and 50 mm in diameter. These specific dimensions were deliberately chosen to meet the requirements for dielectric measurements.

2.3.2 Equipment and test setup

The focus of the investigation shifts to the testing phase, where the Keysight vector network analyzer (Keysight Model: E5080A)[54] plays a prominent role. This technologically advanced device, capable of analyzing frequencies ranging from 200 MHz to 6500 MHz, possesses the capacity to evaluate dielectric properties at various frequencies. The dielectric probe measurement method was employed, utilizing

a coaxial probe to determine the dielectric properties of the paste after mixing. The specimen, enclosed in a container engineered to prevent moisture evaporation, is carefully positioned within the experimental setup. The current scenario is set for the dynamic interplay between the specimen and electromagnetic fields, an event with the potential to unveil intricate aspects of dielectric phenomena.

2.3.3 Measurement and analysis

The rhythm of measurement is initiated immediately after the mixing process, commencing at time zero. This decision ensures that the dielectric properties are tracked from the inception of hydration, capturing the critical early stages of cement's journey toward maturity. A temporal cadence is established, with measurements scheduled at regular 30-minute intervals, spanning the entire 360-minute (6-hour) duration. This temporal granularity unravels the dynamic narrative of dielectric behavior, offering insights into how the material's responses evolve.

The core of the investigation lies in measuring and subsequently analyzing the dielectric properties, specifically the dielectric constant (ε') and the loss tangent ($tan\ \delta$). As the vector network analyzer takes the lead, reflection coefficient measurements ensue. This performance extracts the fundamental data to decode the material's response to electric fields. The data collection process was facilitated and analyzed using ORIGINPRO 2020 software. This software enabled a streamlined analysis process by integrating all required computations and graphical representations into a singular software environment.

The complex (electric) permittivity ε^*, which consists of real and imaginary parts of the capacitance, is defined by the relationship expressed in Eq. (2):

$$\varepsilon^* = \varepsilon' - j\,\varepsilon'' \tag{2}$$

Here, ε' and ε'' represent the real and imaginary components of the capacitance, respectively, within the complex permittivity framework, where j is defined as $\sqrt{-1}$. The real part, also known as the dielectric constant, ε', measures the energy transferred from an external electric field and stored in a material. The imaginary part, ε'', measures how lossy a material is to an external electric field and is referred to as the relative loss factor.

In parallel, the loss tangent ($tan\ \delta$) emerges as an indicator of the material's energy dissipation capability. It is derived from the interplay of the real part of capacitance (ε') and its imaginary counterpart (ε''). The $tan\ \delta$ represents the material's ability to transform energy within an electric field and is expressed in Eq. (3):

$$tan\ \delta = (\varepsilon''/\varepsilon') \tag{3}$$

These parameters are deciphered and recorded for each sample at regular intervals, typically every 30 minutes over 360 minutes (6 hours), providing a dynamic profile of how the dielectric properties evolve. The analysis considers both systematic mistakes, which might arise from the instrumentation and measurement techniques, and random errors, which are likely produced by sample heterogeneity and environmental fluctuations during testing. Repeatability tests were performed on crucial studies to assess the consistency of the outcomes. Furthermore, we employed statistical methods to determine the uncertainty bounds for our measurements and quantify the associated mistakes. This approach improves the accuracy of our conclusions on the dielectric characteristics of hydraulic cement paste. As shown in Fig. 5, a flowchart summarizing the statistical models that were devised for the dielectric process and behavior.

3. Experimental results and statistical modeling

3.1 Dielectric properties of eco-efficient cement-fly ash pastes

The investigation into the dielectric properties of mix FA10, characterized by a 10 wt% replacement of cement with fly ash, reveals intriguing insights into the evolving nature of its dielectric constant at various frequencies over 360 minutes, as shown in Fig. 6(a). As we traverse the frequency spectrum from 200 to 6500 MHz, distinct patterns emerge in the dielectric constant values over time. At 200 MHz, the initial dielectric constant stands at 51.05 F/m, experiencing a gradual decline over the first 30 minutes to stabilize around 41.01 F/m. The subsequent intervals showcase a minor but consistent upward trend, culminating in a value of 48.55 F/m at the 360-minute mark. This frequency-specific behavior suggests a dynamic interplay between the electromagnetic fields and the evolving microstructure,[4–5,7] potentially influenced by the hydration process and the interactions between cement and fly ash.[1,39,47]

Within each frequency band, the FA10 mix unravels intriguing temporal trends. For example, at the 1000 MHz frequency, the dielectric constant starts at 47.57 F/m and experiences a gradual descent within the initial 30 minutes, reaching 38.08 F/m. The subsequent time intervals witness incremental increases, steadying at 44.16 F/m at 360 minutes. This time-dependent variability underscores the dynamic evolution of the material's microstructure and chemical composition during hydration.[9] As the frequency continues to increase, similar trends are observed. At 2000 MHz, the dielectric constant starts at 46.22 F/m and decreases to 42.78 F/m after 360 minutes (6 hours). The same pattern persists across 3000 MHz, 4000 MHz, 5000 MHz, 6000 MHz, and 6500 MHz, with corresponding final dielectric constant values between 41.63 F/m and 37.48 F/m.

The observed trends offer insight into interactions within the mix of FA10. The initial drop in the dielectric constant could be attributed to factors like initial water absorption, pore filling, and the establishment of the electrical double layer.[3,7,15] The subsequent upward trends signify the progression of hydration, crystallization, and the development of internal structures that influence the dielectric response[17,18,33,55-58] These trends reflect the changes in conductivity, mobility of ions, and relaxation phenomena occurring within the cementitious matrix. While the dielectric constant values

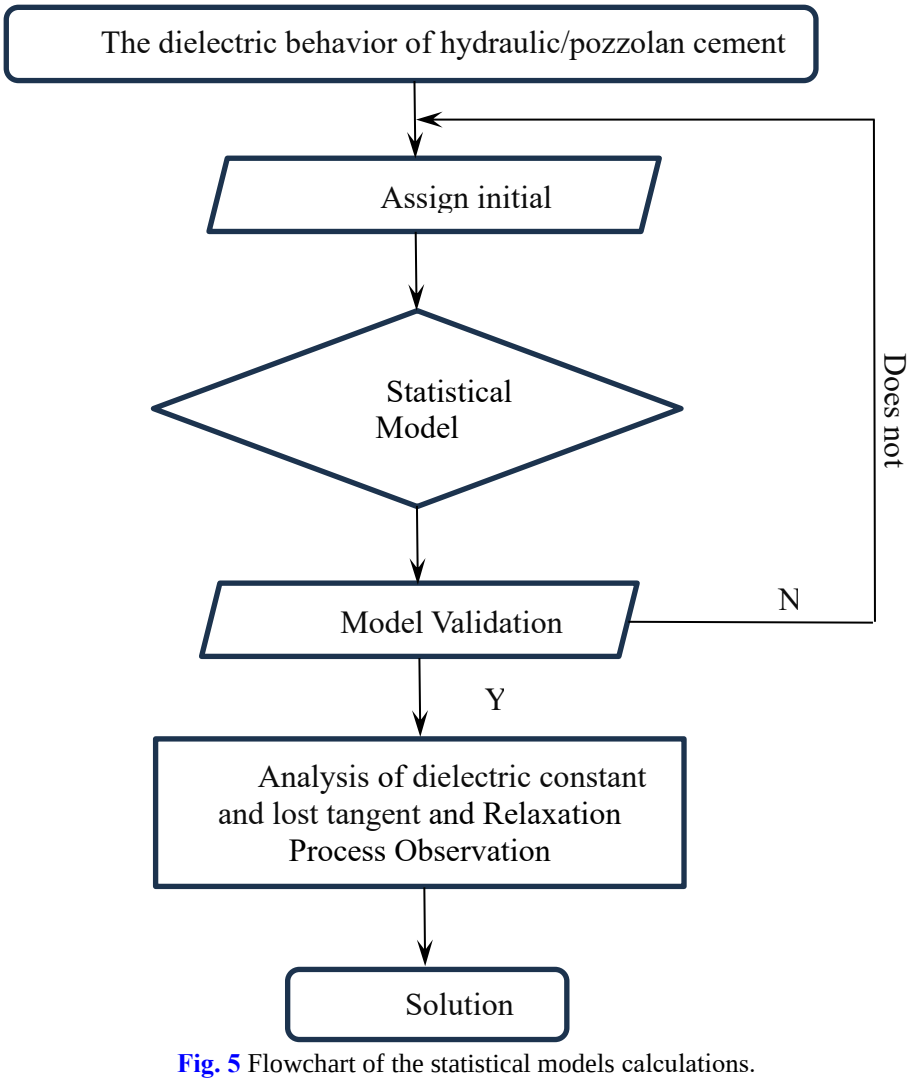

Fig. 5 Flowchart of the statistical models calculations.

provide a quantitative snapshot of energy storage capabilities, the nuanced trends and temporal variations reveal the material's hidden narratives. Though rooted in electromagnetic force revelations, they embrace material science, offering insights into hydration kinetics, microstructural evolution, and potential correlations with mechanical properties.[16,31]

The loss tangent values obtained for mix FA10 offer intriguing insights into the material's dielectric behavior and energy dissipation characteristics.[17,34] The loss tangent values at various frequencies provide information about the material's ability to dissipate energy through heat during electromagnetic interactions, as shown in Fig. 6(b). At a frequency of 200 MHz, the loss tangent values begin at 2.55 and gradually increase over the testing duration, reaching 3.31 at 360 minutes. This trend indicates a slight rise in energy dissipation capacity, suggesting that electromagnetic interactions result in limited energy loss through heat generation. A consistent pattern emerges when examining higher frequencies, such as 1000 MHz, 2000 MHz, and beyond. The loss tangent values exhibit a minor upward trend. For instance, at 1000 MHz, the values start at 0.63 and progress to 0.82. This trend indicates increased energy dissipation capabilities at higher frequencies, albeit at relatively low levels.[17,18]

The behavior of the loss tangent values reflects the inherent nature of fly ash as a supplementary cementitious material. The addition of fly ash contributes to increased porosity, thereby promoting the movement of ions and enabling a degree of energy dissipation during electromagnetic interactions.[28,31,37,56,58] However, the relatively low values of the loss tangent suggest that the energy dissipation capacity of mix FA10 is small. Comparing these results to the dielectric constant values, it is clear that there is a positive correlation between the material's energy storage (ε') and energy dissipation ($tan\ \delta$) capacities. These properties increase as the material undergoes hydration and chemical reactions, indicating dynamic changes within the cementitious matrix.

In the investigation of the relationship between frequency (f) and hydration time (t) on the dielectric constant (ε') value of cement paste for FA10, we employed a 2D polynomial model to establish a comprehensive understanding of this complex interaction, as shown in Table 4. This statistical model allows us to analyze the combined impact of frequency and hydration

time on the dielectric constant value of the cement paste. This analysis serves as a valuable tool for optimizing the properties of cement paste to suit a wide range of applications. The model is expressed as a polynomial equation in two dimensions, with both frequency (f) and hydration time (t) considered independent variables. The equation includes terms up to the fifth order for both variables, capturing potential non-linear effects that may influence the dielectric constant.

The parameters extracted from the model provide insights into the magnitude and nature of frequency and hydration time contributions to the dielectric constant. Notably, the intercept term, z0, has been determined to be 52.39228 with a relatively small uncertainty of ± 0.17351. The magnitudes of these coefficients indicate the strength and direction of the effect, with this value representing the baseline dielectric constant when both frequency and hydration time are zero and the coefficients A_1 to A_5 and B_1 to B_5 reflecting the degree of influence of frequency and hydration time, respectively. For instance, negative coefficients like A_1 (-9.50211×10^{-9}) and B_1 (-0.35675) suggest a decrease in dielectric constant with increasing frequency and hydration time, respectively.

The reduced chi-square value of 0.72959 indicates a strong fit of the model to the data, signifying that the selected polynomial 2D equation effectively captures the variations in the dielectric constant as a function of frequency and hydration time. The R-square value of 0.91724 suggests that the model can explain approximately 91.7% of the variance in the dielectric constant, affirming its predictive capability. Furthermore, the adjusted R-square value of 0.91692 underscores the model's robust explanatory power, accounting for the number of predictor variables.

$$\epsilon'(f,t) = z0 + A_1 f + A_2 f^2 + A_3 f^3 + A_4 f^4 + A_5 f^5 + B_1 t + B_2 t^2 + B_3 t^3 + B_4 t^4 + B_5 t^5 \quad (4),$$

where, ε' is the dielectric constant (F/m), f is the frequency (Hz), and t is the hydration time (min).

The rational 2D model developed for FA10's loss tangent provides valuable insights into the complex interactions between frequency, hydration time, and the material's electrical properties, as shown in Table 5. Each coefficient plays a unique role in shaping the behavior of the loss tangent value.

The equation's constant term (z0) represents the loss tangent at the reference frequency and hydration time, reflecting the inherent material properties unaffected by external factors. Coefficients A_1, A_2, A_3, and A_4 introduce frequency-independent effects associated with hydration time. Notably, A_2 (0.14015) suggests that hydration time influences the loss tangent non-linearly.

Coefficients A_1 to A_3 introduce frequency-dependent effects on the loss tangent. The positive value of A_1 (8.51683×10^{-8}) suggests an increase in the loss tangent with

Table 4. The statistical model for predicting dielectric constant values of 90 wt% eco-efficient cement-10 wt% fly ash paste.

z0	A_1	A_2	A_3	A_4	A_5
52.39228 ± 0.17351	-9.50211E-9 ± 4.4555E-10	5.40559E-18 ± 3.8635E-19	-1.56163E-27 ± 1.41943E-28	2.11653E-37 ± 2.31096E-38	-1.09753E-47 ± 1.3735E-48
R^2	B_1	B_2	B_3	B_4	B_5
0.91692	-0.35675 ± 0.00381	0.00564 ± 7.27694E-5	-3.51814E-5 ± 5.35032E-7	9.61956E-8 ± 1.66303E-9	-9.59075E-11 ± 1.83855E-12

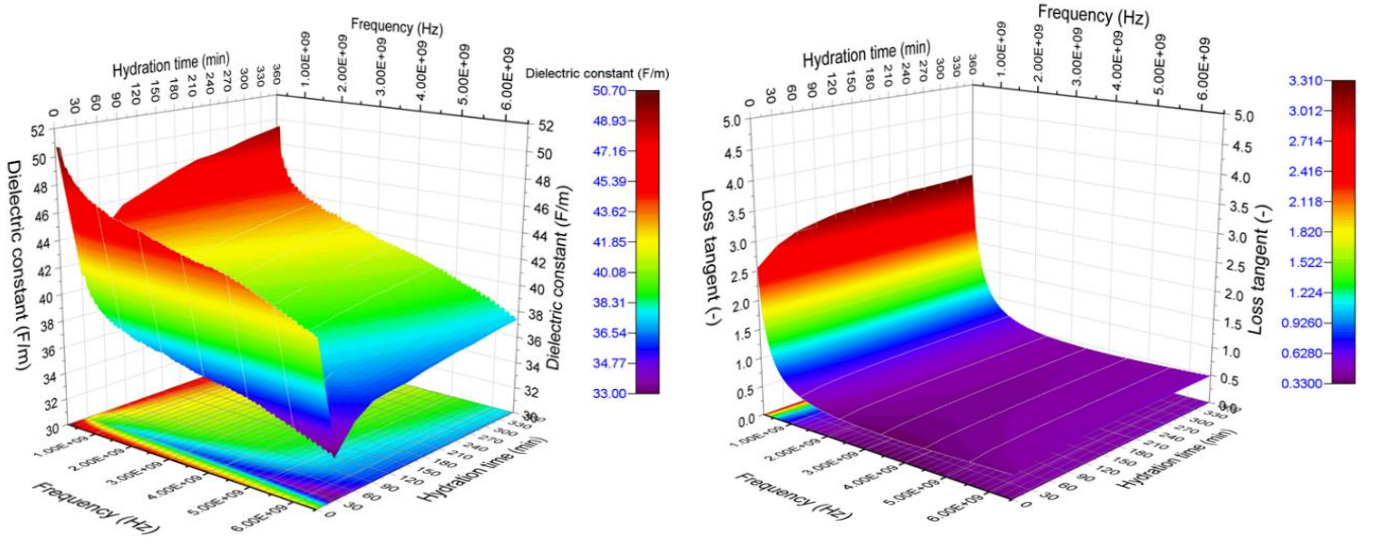

(a) Dielectric constant (ε') (b) Loss tangent ($tan\ \delta$)

Fig. 6 The 3D graph illustrating the simultaneous influence of frequency and hydration time on the dielectric constant and loss tangent of 90 wt% eco-efficient cement-10 wt% fly ash paste.

Table 5. The statistical model for predicting loss tangent values of 90 wt% eco-efficient cement-10 wt% fly ash paste.

z0	A_1	A_2	A_3	A_4	A_5
44.79868 ± 2.89282	1.23327E-9 ± 2.1587E-10	0.14015 ± 0.01034	-5.6224E-4 ± 4.01552E-5	7.67711E-7 ± 5.32773E-8	-
R^2	B_1	B_2	B_3	B_4	B_5
0.99945	8.51683E-8 ± 5.77168E-9	-1.56274E-17 ± 9.44985E-19	8.67836E-28 ± 4.6475E-29	3.01041E-4 ± 6.49572E-4	1.53851E-7 ± 1.52926E-6

increasing frequency, potentially due to relaxation mechanisms within the material. Meanwhile, coefficient A_4 captures the impact of hydration time on the loss tangent, with its value (3.01041×10^{-4}) indicating a slight increase in the loss tangent with hydration time. This behavior can be attributed to changes in the microstructure and conductivity of the material during hydration.[18,45]

The model's high accuracy is evident from the reduced chi-square value (8.87481×10^{-5}) and the extremely close R-square value (0.99945) and adjusted R-square (0.99945), indicating an excellent fit between the model and the experimental data, especially considering the number of predictor variables.

$$tan\ \delta(f,t) = \frac{z0+A1f+A_1t+A_2t^2+A_3t^3}{1+B_1f+B_2f^2+B_3f^3+B_4t+B_5t^2} \quad (5),$$

where, $tan\ \delta$ is the loss tangent, f is the frequency (Hz), and t is the hydration time (min).

The dielectric constant values for mix FA30 (30 wt% replacement of eco-cement by fly ash) offer intriguing insights into how introducing a significant proportion of fly ash influences the material's dielectric behavior, as shown in Fig. 7(a).

At 200 MHz, the dielectric constant values consistently remained low throughout the 6-hour monitoring period, maintaining a value of 0.00 F/m. This unique behavior suggests that, at this frequency range, the material's response to an electric field is minimal, possibly due to the specific characteristics of fly ash altering the material's electrical conductivity.[17,36,57,59]

The dielectric constant's behavior changes as the frequency increases to 1000 MHz. Initially measured at 24.61 F/m, the value gradually increases with time, reaching 20.70 F/m after 360 minutes (6 hours).This trend suggests that the material begins to exhibit a capacity for energy storage due to hydration-induced changes in its microstructure and conductivity. Interestingly, the dielectric constant values at this frequency range are significantly lower than those observed in mix FA10. This discrepancy could be attributed to the higher fly ash content in mix FA30, which might impact the distribution of ions and thus affect the dielectric behavior. The dielectric constant across the higher frequency ranges exhibits a consistent upward trend, mirroring the behavior seen at 1000 MHz. This pattern holds for 2000 MHz, 3000 MHz, 4000 MHz, 5000 MHz, 6000 MHz, and 6500 MHz, with dielectric constant values converging toward 20.52 F/m at 6500 MHz.

The behavior observed in mix FA30 underscores the complexity of fly ash's influence on dielectric attributes. The remarkably low dielectric constant values at 200 MHz suggest fly ash significantly dampens the material's response to an electric field at lower frequencies. However, the rise in dielectric constant with increasing frequency indicates that this influence is frequency-dependent, possibly linked to the distribution and mobility of charges within the material. Comparatively, mix FA30 demonstrates a distinct response compared to mix FA10, highlighting the significance of fly ash content in shaping dielectric behavior.[59–61] This mix presents an opportunity to explore how the material's microstructural and electrical properties evolve with increasing fly ash content, paving the way for more profound insights into the pozzolanic contributions of fly ash to cementitious materials' dielectric attributes.

The loss tangent values obtained for the cement paste with a 30 wt% replacement of cement by fly ash (FA30) provide valuable insights into how adding fly ash affects the material's energy dissipation behavior, as shown in Fig. 7(b).

At a frequency of 200 MHz, the loss tangent values consistently remained at 1.00 throughout the entire testing period of 360 minutes. This stability in the loss tangent values could be attributed to the initial stages of the hydration process, where the material is still undergoing significant chemical reactions, resulting in a relatively stable energy dissipation behavior.

As the frequency increases to 1000 MHz, the loss tangent values gradually increase from 0.69 to 0.74. This trend indicates that the energy dissipation capacity of the material increases as the frequency rises, likely due to the increased interactions between the electromagnetic field and the microstructure of the material.[17,28,62].

As we continue to higher frequencies, the loss tangent values steadily rise. At 2000 MHz, the values increase from 0.38 to 0.42; at 3000 MHz, they range from 0.29 to 0.33. This trend suggests that the energy dissipation behavior of the cement paste continues to evolve as the frequency becomes more pronounced, reflecting the dynamic changes within the material's microstructure. The consistent rise in loss tangent values across frequencies indicates that adding fly ash to the cement paste improves energy dissipation capabilities. This improvement could be attributed to the unique properties of fly ash, which can alter the microstructure of the cement matrix and enhance its ability to interact with electromagnetic fields.[27,47,59–61] Comparing these results with the dielectric constant values shows a relationship between energy storage (ε') and energy dissipation ($tan\ \delta$). As the material's energy storage capacity increases, so does its energy dissipation

capacity, likely due to the dynamic changes in its microstructure and chemical composition.

The statistical model provides a comprehensive understanding of the relationship between the dielectric constant, frequency, and hydration time for cement paste with a 30 wt% replacement of cement by fly ash (FA30). The equation accounts for both linear and non-linear effects, offering a holistic representation of the material's dielectric behavior, as shown in Table 6.

The constant term (z0), determined to be 3.31769, represents the baseline dielectric constant at the reference frequency and hydration time. The coefficients A_1 to A_5 contribute to the impact of frequency, while B_1 to B_5 contribute to the impact of hydration time. The presence of non-zero coefficients A_1, B_1, B_2, and B_3 indicates that both frequency and hydration time play significant roles in shaping the dielectric properties of FA30 cement paste.

From the coefficient values, it can be inferred that the dielectric constant is positively influenced by the frequency, as indicated by the positive coefficients A_1 to A_5. This influence may be attributed to increased polarization effects at higher frequencies. Conversely, the negative coefficient for B_1 (-0.21266) suggests that longer hydration times result in decreased dielectric constants. This decrease could be due to changes in microstructure or porosity as hydration progresses. The goodness-of-fit measures include an R-square value of 0.86743 and an adjusted R-square value of 0.86692, indicating that the model captures a substantial portion of the variability in the data. Additionally, the reduced chi-square value of 1.14303 indicates that the model adequately describes the observed data.

The rational 2D model crafted for FA30's loss tangent offers profound insights into the interplay of frequency, hydration time, and the material's electrical properties, as shown in Table 7.

The constant term (z0) signifies the loss tangent at a reference frequency and hydration time, with a magnitude of 3.06983×1014pointing to high values indicative of unique behavior within this material. Coefficients A1, A2, A3, and A4 introduce frequency-independent effects associated with hydration time. The magnitudes of A1 and A2 highlight their strong influence on the loss tangent. The negative value of A1(-625979.15189) suggests a reduction in the loss tangent with increasing frequency. Coefficient A1 introduces a frequency-dependent effect. The positive value of A_1 (582070.30898) suggests a rise in the loss tangent with increasing frequency, which is consistent with relaxation mechanisms within the material. Coefficient A_2 captures the quadratic frequency-dependent effect, with its negative value (-0.0052) indicating a curvilinear relationship with frequency. The minimal value of A_3 (1.19034×10^{-11}) suggests a minimal cubic frequency-dependent impact on the loss tangent. Coefficients A_4 and A_5 introduce hydration-time-dependent effects. Their values suggest that hydration time plays a role in shaping loss tangent behavior. The excellent fit between the model and the experimental data is evident from the reduced chi-square value (1.53611), the high R-square (0.93537), and the adjusted R-square (0.93514) values.

Table 6. The statistical model for predicting dielectric constant values of 70 wt% eco-efficient cement-30 wt% fly ash paste.

z0	**A_1**	**A_2**	**A_3**	**A_4**	**A_5**
3.31769 ± 0.21717	4.28995E-8 ± 5.57682E-10	-2.97422E-17 ± 4.83583E-19	9.25739E-27 ± 1.77666E-28	-1.32413E-36 ± 2.89256E-38	7.07916E-47 ± 1.71917E-48
R^2	**B_1**	**B_2**	**B_3**	**B_4**	**B_5**
0.86692	-0.21266 ± 0.00477	0.00302 ± 9.10833E-5	-1.80764E-5 ± 6.69684E-7	4.83766E-8 ± 2.08157E-9	-4.76365E-11 ± 2.30126E-12

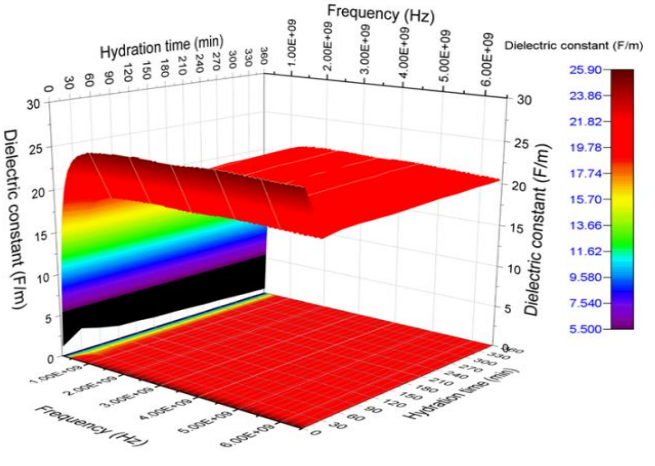

(a) Dielectric constant (ε')

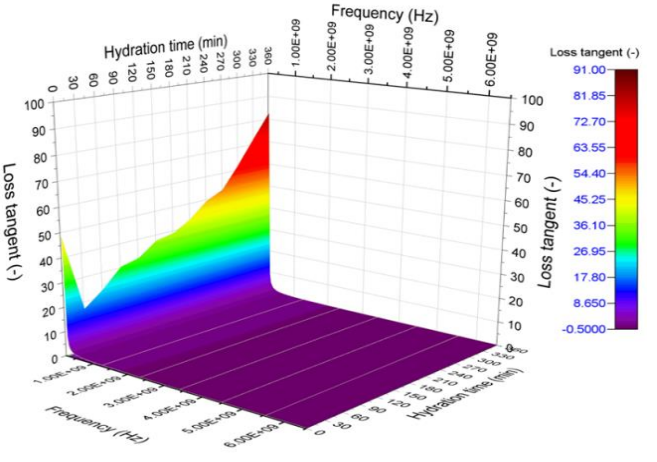

(b) Loss tangent ($tan\ \delta$)

Fig. 7 The 3D graph illustrating the simultaneous influence of frequency and hydration time on the dielectric constant and loss tangent of 70 wt% eco-efficient cement-30 wt% fly ash paste.

Table 7. The statistical model for predicting loss tangent values of 70 wt% eco-efficient cement-30 wt% fly ash paste.

z0	A_1	A_2	A_3	A_4	A_5
3.06983E14 ± 3.64293E13	-625979.15189 ± 125893.06043	-2.02248E12 ± 2.30134E11	2.9632E10 ± 1.68495E9	-6.83491E7 ± 3351170.56028	-
R^2	B_1	B_2	B_3	B_4	B_5
0.93514	582070.30898 ± 3943.20774	-0.0052 ± 2.08863E-5	1.19034E-11 ± 4.79865E-14	8.90192E10 ± 4.38839E9	-2.64908E8 ± 1.19799E7

3.2 Dielectric properties of eco-efficient cement-calcium carbonate pastes

The dielectric constant values revealed for CC10, with a 10 wt% replacement of cement by calcium carbonate, offer intriguing insights into the material's dielectric behavior under the influence of this pozzolan, as shown in Fig. 8(a). At 200 MHz, the dielectric constant values consistently remain low, registering at 0.00 F/m across all time intervals. This observation hints at a unique electromagnetic interaction pattern at this frequency. As the frequency escalates to 1000 MHz, a shift occurs in the behavior of the dielectric constant, which starts at 33.41 F/m. The values exhibit a downward trend over the initial 90-minute interval, reaching 29.22 F/m. This decline suggests a diminishing capacity for energy storage within the material, potentially influenced by initial hydration reactions and microstructural changes.[31,34]

The behavior takes an intriguing twist as the frequency reaches 2000 MHz and beyond. The dielectric constant values rise, starting at 38.00 F/m and gradually increasing to 51.57 F/m at 2000 MHz. This peculiar behavior signifies an evolving capacity for energy storage as time progresses. The upward trend continues as the frequency reaches 3000 MHz, 4000 MHz, 5000 MHz, 6000 MHz, and 6500 MHz, with dielectric constant values ranging from 55.78 F/m to 56.11 F/m. The remarkable behavior at higher frequencies suggests a dynamic evolution of the material's electromagnetic interactions, potentially influenced by the evolving microstructure and conductivity due to hydration reactions. Notably, the transition from a declining trend to an ascending trend around 2000 MHz indicates a critical point at which the material's electromagnetic behavior transforms. This intriguing trend could be attributed to the interplay between the electromagnetic field and the evolving calcium carbonate-laden microstructure. The porosity and connectivity of the matrix, influenced by the unique properties of calcium carbonate, could contribute to the observed behavior.[1]

The loss tangent values obtained for cement paste mix CC10, which involves a 10 wt% replacement of cement with calcium carbonate across different frequencies and durations, are shown in Fig. 8(b). At the lowest frequency of 200 MHz, the loss tangent values remain constant at 1.00 throughout the entire 360-minute testing period. This unchanging trend suggests that the material exhibits consistent energy dissipation characteristics at this frequency range, indicating a minimal ability to absorb and dissipate electromagnetic energy. As the frequency increases to 1000 MHz, the loss tangent values substantially rise from 0.98 to 2.51 over the testing duration. This significant increase in the loss tangent values reflects an enhanced ability of the material to dissipate energy at higher frequencies. This trend implies that the material's microstructure undergoes adjustments that facilitate increased energy dissipation capabilities.[27,28] At higher frequencies (2000 MHz and beyond), the loss tangent values experience a more gradual increase, moving from 0.49 to 0.92. These increments indicate continued improvements in energy dissipation behavior, although the enhancement rate slows as the frequency increases.

In the context of Cement Paste mix CC10, the constant loss tangent values at lower frequencies (200 MHz) suggest a consistent behavior with limited energy dissipation abilities. However, the sharp increase in loss tangent values at 1000 MHz demonstrates that this mix becomes more effective at dissipating energy as the frequency rises. This increase in effectiveness could be attributed to the microstructural changes induced by calcium carbonate, which might affect how the material interacts with electromagnetic fields.[63] The observed trend of increasing loss tangent values with frequency is typical of many materials and indicates their ability to absorb and dissipate energy from electromagnetic waves. The significant enhancement in energy dissipation at higher frequencies could make cement paste mix CC10 particularly useful for applications where electromagnetic interference mitigation is necessary.

The statistical model provides valuable insights into the relationship between frequency, hydration time, and the dielectric constant of CC10, as shown in Table 8. The constant term (z0) represents the dielectric constant at the reference frequency and hydration time. The coefficients A_1 to A_5 capture the frequency-dependent effects on the dielectric constant. Notably, the positive value of A_1 (6.44681×10^{-8}) indicates that an increase in frequency leads to an increment in the dielectric constant. This frequency dependence may be attributed to enhanced polarization mechanisms within the material.[28,30,31]

The coefficients B_1 to B_5 correspond to the influence of hydration time on the dielectric constant. A positive coefficient for B_1 (0.17929) suggests that longer hydration times result in higher dielectric constants. This phenomenon could be linked to structural changes within the material as it undergoes hydration, affecting its dielectric properties. The statistical model's effectiveness is evident from the reduced chi-square value (14.03971), which suggests that the model adequately represents the observed data. The high R-square value (0.94315) and adjusted R-square (0.94294) indicate that

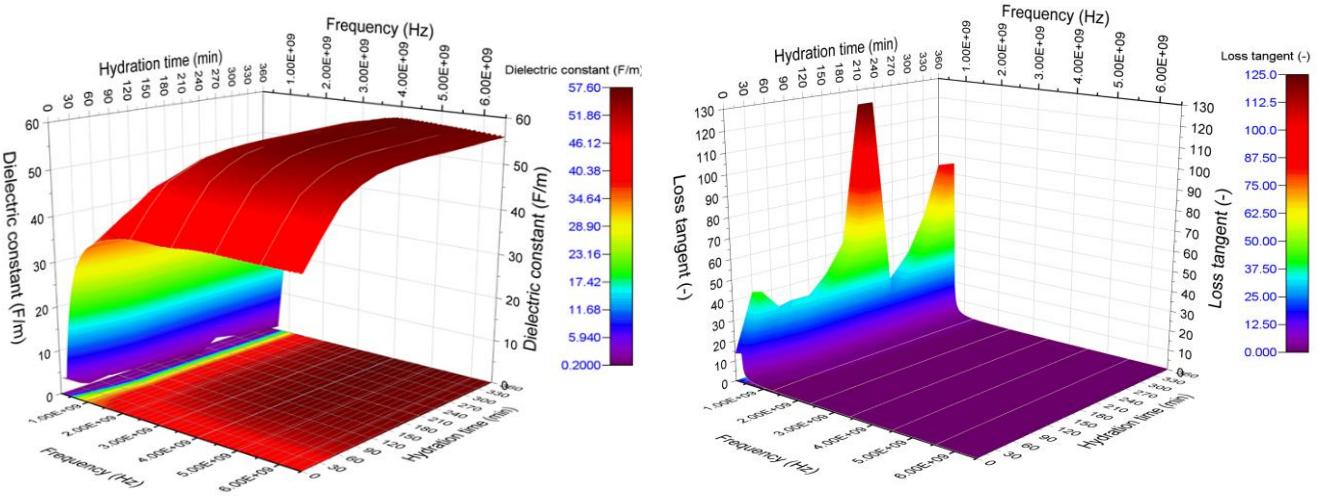

(a) Dielectric constant (ε') (b) Loss tangent ($tan\ \delta$)

Fig. 8 The 3D graph illustrating the simultaneous influence of frequency and hydration time on the dielectric constant and loss tangent of 90 wt% eco-efficient cement-10 wt% calcium carbonate paste.

Table 8. The statistical model for predicting dielectric constant values of 90 wt% eco-efficient cement-10 wt% calcium carbonate paste.

z0	**A_1**	**A_2**	**A_3**	**A_4**	**A_5**
-30.11839 ± 0.76112	6.44681E-8 ± 1.95451E-9	-1.76499E-17 ± 1.69481E-18	9.39579E-28 ± 6.22667E-28	2.58528E-37 ± 1.01375E-37	-2.76984E-47 ± 6.02516E-48
R^2	**B_1**	**B_2**	**B_3**	**B_4**	**B_5**
0.94294	0.17929 ± 0.01671	-0.00104 ± 3.19219E-4	2.76547E-6 ± 2.34704E-6	-3.06421E-9 ± 7.29527E-9	7.31756E-13 ± 8.06522E-12

the model can explain a substantial portion of the dielectric constant variability.

The polynomial 2D model for the loss tangent of CC10 provides valuable insights into the interplay between frequency, hydration time, and the material's electrical properties, as shown in Table 9. The constant term (z0) represents the baseline loss tangent at a reference frequency and hydration time. With a magnitude of 82.70311, this term indicates the material's intrinsic electrical properties. The coefficients A_1 to A_5 capture frequency-dependent effects on the loss tangent. The negative value of A_1 (-1.44553×10^{-7}) suggests that an increase in frequency may decrease the loss tangent. The subsequent coefficients, A_2 to A_5, introduce higher-order frequency-dependent behaviors, but their extremely small magnitudes (-1.7251×10^{-46} to 8.92127×10^{-17}) suggest minimal contributions.

Coefficients B_1 to B_5 introduce hydration-time-dependent effects. The small value of B_1 (0.05881) indicates that hydration time is limited in shaping the loss tangent behavior for CC10. The reduced chi-square value (81.23146) indicates that the model might not perfectly fit the data, and the relatively low R-square (0.61305) and adjusted R-square (0.61157) values suggest that the model explains only a portion of the variance in the data.

The dielectric constant values unveiled for mix CC30 present a captivating narrative of how a higher dosage of calcium carbonate as a pozzolan influences the material's dielectric behavior, as shown in Fig. 9(a). At 200 MHz, the dielectric constant remains consistently at 0.00 F/m throughout the 360-minutes (6-hours) timeframe, suggesting a limited energy storage capacity at this frequency. As the frequency increases to 1000 MHz, an intriguing trend emerges in the dielectric constant values. Its values start at 23.74 F/m, exhibit fluctuations, and follow an overall declining pattern over time, reaching a minimum of 12.79 F/m at 360 minutes. This profound drop signifies a substantial alteration in the

Table 9. The statistical model for predicting loss tangent values of 90 wt% eco-efficient cement-10 wt% calcium carbonate paste.

z0	**A_1**	**A_2**	**A_3**	**A_4**	**A_5**
82.70311 ± 1.83079	-1.44553E-7 ± 4.70132E-9	8.92127E-17 ± 4.07666E-18	-2.54473E-26 ± 1.49775E-27	3.40226E-36 ± 2.43846E-37	-1.7251E-46 ± 1.44928E-47
R^2	**B_1**	**B_2**	**B_3**	**B_4**	**B_5**
0.61157	0.05881 ± 0.04019	-0.00106 ± 7.67843E-4	1.03566E-5 ± 5.64551E-6	-4.05446E-8 ± 1.75479E-8	5.29943E-11 ± 1.93999E-11

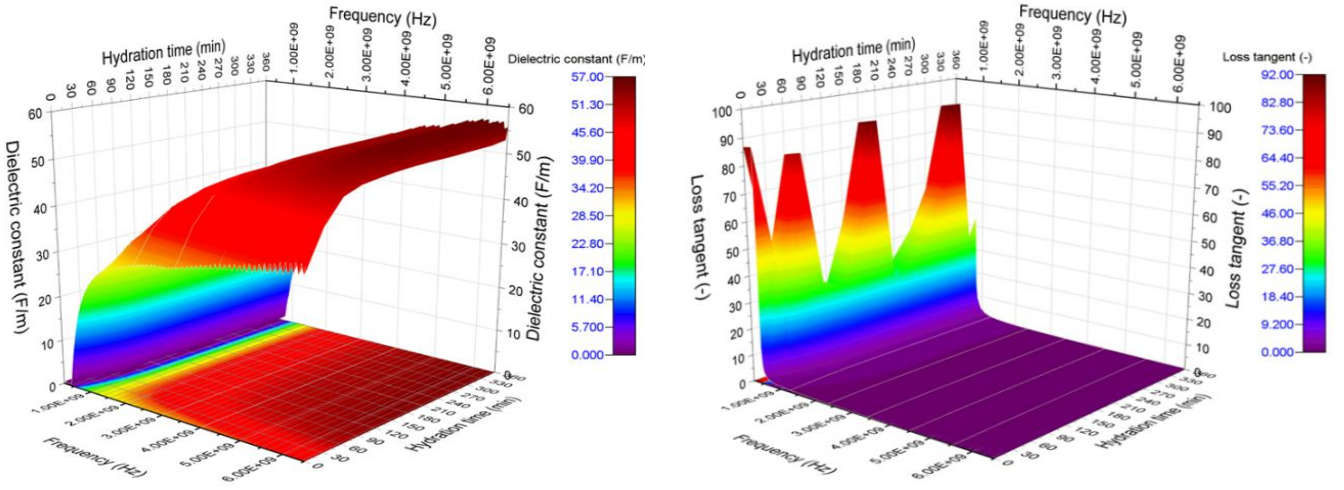

(a) Dielectric constant (ε')

(b) Loss tangent ($tan\ \delta$)

Fig. 9 The 3D graph illustrates the simultaneous impact of frequency and hydration time on the dielectric constant and loss tangent of 70 wt% eco-efficient cement-30 wt% calcium carbonate paste.

material's energy storage capacity, likely tied to hydration-induced microstructural transformations.

Interestingly, as the frequency continues to rise to 2000 MHz, 3000 MHz, 4000 MHz, 5000 MHz, 6000 MHz, and 6500 MHz, the dielectric constant values showcase a reversal of the previous trend. Instead of decreasing, the values consistently increased over 6 hours. This unique behavior suggests that the material's energy storage capacity becomes more pronounced at higher frequencies as the hydration process progresses.[31,35]

The dynamic trend in dielectric constant values at different frequencies highlights the intricate interactions between calcium carbonate and the electromagnetic field. The progressive rise in values at higher frequencies could stem from a combination of pore structure changes and ion mobility influenced by the calcium carbonate content.[63,64] The contrast in behavior between lower and higher frequencies underscores the complex and multifaceted nature of the material's evolving electrical characteristics. Mix CC30 stands out for its intricate and contrasting behavior compared to the other mixes explored. While mix FA10 and mix FA30 demonstrated decreasing and increasing trends, mix CC10 displayed increasing trends at all frequencies. Mix CC30 displayed decreasing values at 1000 MHz, followed by an upward trend at higher frequencies. The blend of frequency-dependent trends reflects the material's evolving microstructure, influenced by the interaction between calcium carbonate and the ongoing hydration reactions.[63,64]

The loss tangent values obtained for CC30 provide valuable insights into its energy dissipation behavior across various frequencies and durations, as shown in Fig. 9(b). The loss tangent values at a frequency of 200 MHz remain consistently high at 1.00 throughout the entire 360-minute testing period. This constant behavior suggests that CC30 exhibits minimal energy dissipation capabilities, irrespective of time and frequency. As the frequency increases to 1000 MHz, the loss tangent values display an exciting and significant trend. Starting at 1.06, they consistently rise to 3.90 by the end of the testing period. This substantial increase signifies an enhancement in the material's energy dissipation capabilities over time, particularly at this frequency range. The gradual rise in loss tangent values implies that CC30 might undergo microstructural changes that improve its energy dissipation abilities. The pronounced increase in loss tangent values indicates that the material might be well-suited for applications involving higher frequencies that demand efficient energy dissipation.[4,7,10]

When the frequency increases to 2000 MHz and beyond, the loss tangent values increase incrementally, ranging from 0.42 to 1.02. This upward trend suggests that the material's energy dissipation capabilities become more pronounced at higher frequencies, aligning with the growing loss tangent values observed. CC30's constant loss tangent value of 1.00 at lower frequencies indicates a consistently limited ability to dissipate energy. However, the significant increase in loss tangent values at higher frequencies (1000 MHz) demonstrates improved energy dissipation performance. This increase indicates that CC30 has the potential to be an effective energy dissipator in scenarios involving high-frequency applications. The rising trend in loss tangent values indicates favorable microstructural properties within the mix, enabling enhanced energy dissipation capabilities.

Table 10 shows that the statistical model offers valuable insights into the intricate relationship between frequency, hydration time, and the dielectric constant of CC30. The constant term (z0) represents the dielectric constant at the reference frequency and hydration time. The coefficients A_1 to A_5 capture the frequency-dependent effects on the dielectric constant. Notably, the positive value of A_1 (1.77312×10^{-8}) indicates that an increase in frequency leads to an increment in the dielectric constant. This frequency dependence may arise from enhanced polarization mechanisms within the

Table 10. The statistical model for predicting dielectric constant values of 70 wt% eco-efficient cement-30 wt% calcium carbonate paste

z0	A_1	A_2	A_3	A_4	A_5
-17.91215 ± 0.67257	1.77312E-8 ± 1.7271E-9	1.38084E-17 ± 1.49762E-18	-8.18099E-27 ± 5.50219E-28	1.48671E-36 ± 8.95803E-38	-9.02588E-47 ± 5.32414E-48
R^2	B_1	B_2	B_3	B_4	B_5
0.95849	0.25219 ± 0.01476	-0.00247 ± 2.82078E-4	1.19696E-5 ± 2.07396E-6	-2.79363E-8 ± 6.44646E-9	2.50741E-11 ± 7.12683E-12

material.[13,45]

The coefficients B_1 to B_5 correspond to the influence of hydration time on the dielectric constant. A positive coefficient for B_1 (0.25219) suggests that longer hydration times result in higher dielectric constants. Structural changes within the material during hydration may contribute to this behavior.[7] The reduced chi-square value (10.96273) underscores the statistical model's effectiveness, indicating a good fit between the model and observed data. The high R-square value (0.95864) and adjusted R-square (0.95849) indicate that the model can explain a substantial portion of the dielectric constant variability.

The polynomial 2D model developed for CC30's loss tangent provides valuable insights into the material's electrical behavior, considering both frequency and hydration time, as displayed in Table 11. The constant term (z0) represents the loss tangent at a reference frequency and hydration time. The relatively high value of z0 (89.79483) indicates that CC30 exhibits higher loss tangent behavior than other mixtures. Coefficients A_1 to A_5 introduce frequency-dependent effects. The negative value of A_1 (-1.40873×10^{-7}) implies a decrease in the loss tangent with increasing frequency. The magnitudes of A_2 to A_5 indicate the influence of higher-order frequency-dependent effects on the material's loss tangent.

Coefficient B_1 represents a hydration-time-dependent effect. Its negative value (-0.08008) suggests a decrease in the loss tangent with prolonged hydration time, while coefficients B_2 to B_5 account for higher-order hydration-time-dependent effects. These coefficients highlight the intricate relationship between hydration time and the loss tangent for CC30. The model's goodness of fit can be evaluated using the reduced chi-square value (88.60169), the R-square (0.64825), and the adjusted R-square (0.6469) values. These values indicate that the model captures a substantial portion of the variance in the data. However, the relatively high reduced chi-square value suggests some degree of uncertainty or noise in the model.

3.3 Dielectric properties of eco-efficient cement-diatomite pastes

The dielectric constant values for mix DM10 (10 wt% replacement of cement by diatomite) provide intriguing insights into the influence of diatomite as a pozzolan on the material's dielectric behavior, as shown in Fig. 10(a). At 200 MHz, the dielectric constant remains consistently low, registering at 0.00 F/m, indicating minimal energy storage capacity at this frequency.

As the frequency increases to 1000 MHz, a discernible trend is observed in the dielectric constant values. They start at 28.66 F/m and gradually increase, reaching 31.52 F/m after 360-minutes (6-hours). This upward trend suggests a dynamic shift in the material's energy storage capabilities, potentially driven by microstructural changes resulting from hydration processes.[16,20] Interestingly, at 2000 MHz, 3000 MHz, 4000 MHz, 5000 MHz, 6000 MHz, and 6500 MHz, the dielectric constant values exhibit a distinctive pattern. They consistently increased over 360 minutes (6 hours), ranging from 55.03 F/m to 60.28 F/m. This behavior indicates an evolving capacity for energy storage within the material due to microstructural and conductive changes facilitated by the presence of diatomite.[30]

The frequency-dependent increase in dielectric constant values highlights the intricate relationship between electromagnetic interactions and evolving material characteristics. This trend signifies the evolving response of the material to the electromagnetic field, shaped by its composition, pore structure, and ongoing hydration reactions. Mix DM10 presents a unique profile compared to the earlier mixes involving different pozzolans and replacement levels. The increasing trend in dielectric constant values at all frequencies underscores the evolving electrical behavior and energy storage potential influenced by the addition of diatomite.[65,66]

The loss tangent values for mix DM10 offer valuable insights into its energy dissipation behavior across various frequencies and durations, as shown in Fig. 10(b). At a frequency of 200 MHz, the loss tangent values are uniformly maintained at 1.00 throughout the entire 360-minute testing

Table 11. The statistical model for predicting loss tangent values of 70 wt% eco-efficient cement-30 wt% calcium carbonate paste.

z0	A_1	A_2	A_3	A_4	A_5
89.79483 ± 1.91204	-1.40873E-7 ± 4.90997E-9	8.12859E-17 ± 4.25758E-18	-2.19309E-26 ± 1.56422E-27	2.7983E-36 ± 2.54668E-37	-1.36362E-46 ± 1.5136E-47
R^2	B_1	B_2	B_3	B_4	B_5
0.6469	-0.08008 ± 0.04197	0.00261 ± 8.0192E-4	-2.39008E-5 ± 5.89606E-6	8.50525E-8 ± 1.83267E-8	-1.03294E-10 ± 2.02609E-11

period. This consistent value indicates that the material exhibits stable energy dissipation behavior at this frequency range and does not vary over time. As the frequency increases to 1000 MHz, the loss tangent values show an increasing trend, starting at 0.71 and rising to 2.22 by the end of the testing period. This trend suggests that the energy dissipation capabilities of the material become more pronounced at higher frequencies and over time. The higher frequency loss tangent values indicate enhanced energy dissipation potential, which could be attributed to the interaction between diatomite particles and the cement matrix.

The loss tangent values exhibit incremental changes as the frequency rises to 2000 MHz and beyond. The gradual increase in loss tangent values, moving from 0.37 to 0.86, indicates favorable energy dissipation behavior as the frequency increases. This trend aligns with the previously observed rising loss tangent values, indicating an effective energy dissipation mechanism within the material as frequency increases. The loss tangent values of DM10 indicate that the presence of diatomite in the eco-efficient cement paste enhances its energy dissipation properties, especially at higher frequencies.[32,37] As frequency rises, the increasing trend in loss tangent values points towards improved energy dissipation capabilities, mking DM10 suitable for applications involving higher frequency loading or dynamic stresses.

Table 12 presents the statistical model, which offers a profound understanding of the intricate interactions between frequency, hydration time, and the dielectric constant of DM10. The constant term (z0) represents the dielectric constant at the reference frequency and hydration time. The coefficients A_1 to A_5 capture the frequency-dependent effects on the dielectric constant. The positive value of A_1 (7.71629×10^{-8}) suggests that the dielectric constant increases with frequency. This frequency dependence could arise from material polarization phenomena and other complex interactions.[4,46,67] The coefficients B_1 to B_5 correspond to the effects of hydration time on the dielectric constant. A positive coefficient for B_1 (0.05677) indicates that longer hydration times are associated with higher dielectric constants. The structural changes during hydration and the evolving microstructure of the material could contribute to this behavior.[5,7–9] The reduced chi-square value (31.35087) supports the model's robustness, suggesting a reasonable agreement between the model and the observed data. The relatively high R-square value (0.89824) and adjusted R-square (0.89785) indicate that the model can explain a substantial portion of the dielectric constant's variance.

The polynomial 2D model developed for DM10's loss tangent provides valuable insights into the material's electrical behavior, considering both frequency and hydration time, as shown in Table 13. The constant term (z0) represents the baseline loss tangent at a reference frequency and hydration time, with a value of 70.8437, indicating moderate loss tangent behavior within DM10. Coefficients A_1 to A_5 account for frequency-dependent effects, with the negative value of A_1 (-1.30729×10^{-7}) suggesting a reduction in the loss tangent as

Table 12. The statistical model for predicting dielectric constant values of 90 wt% eco-efficient cement-10 wt% diatomite paste.

z0	A_1	A_2	A_3	A_4	A_5
-40.82283 ± 1.13737	7.71629E-8 ± 2.92067E-9	-2.80901E-17 ± 2.5326E-18	4.44001E-27 ± 9.30468E-28	-2.61929E-37 ± 1.51488E-37	7.47541E-49 ± 9.00357E-48
R^2	B_1	B_2	B_3	B_4	B_5
0.89785	0.05677 ± 0.02497	0.00426 ± 4.77018E-4	-3.82704E-5 ± 3.50724E-6	1.17908E-7 ± 1.09015E-8	-1.23413E-10 ± 1.20521E-11

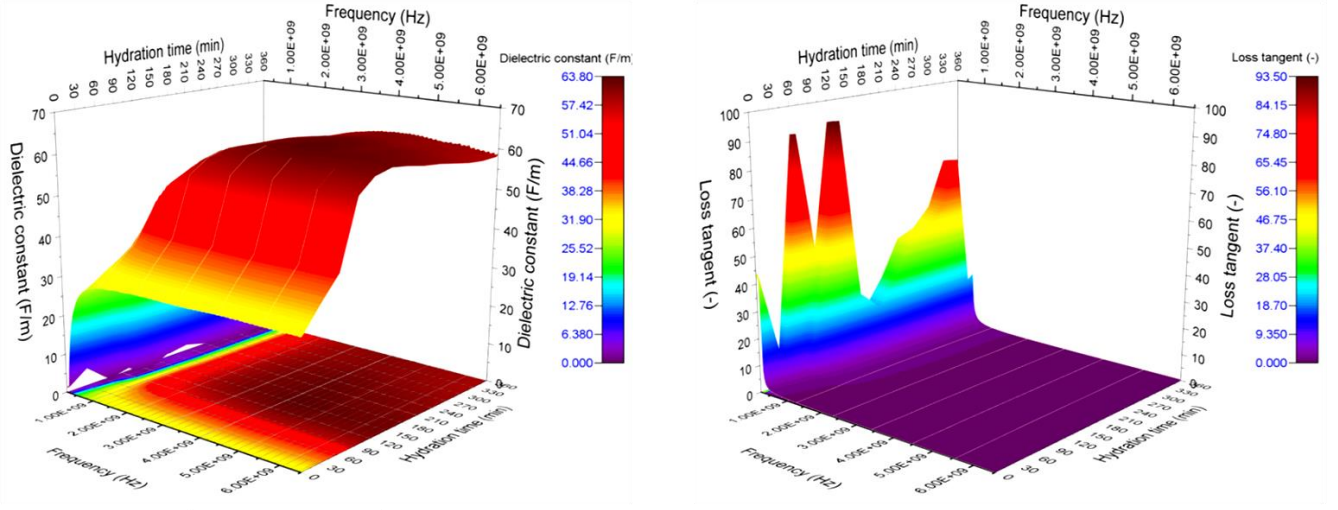

(a) Dielectric constant (ε') (b) Loss tangent ($tan\ \delta$)

Fig. 10 The 3D graph illustrating the simultaneous impact of frequency and hydration time on the dielectric constant and loss tangent of 90 wt% eco-efficient cement-10 wt% diatomite paste.

Table 13. The statistical model for predicting loss tangent values of 90 wt% eco-efficient cement-10 wt% diatomite paste.

z0	A_1	A_2	A_3	A_4	A_5
70.8437 ± 1.56078	-1.30729E-7 ± 4.00796E-9	8.43531E-17 ± 3.47542E-18	-2.49228E-26 ± 1.27686E-27	3.42735E-36 ± 2.07883E-37	-1.77811E-46 ± 1.23554E-47
R^2	B_1	B_2	B_3	B_4	B_5
0.59078	-0.02634 ± 0.03426	0.00204 ± 6.546E-4	-2.09281E-5 ± 4.8129E-6	7.72839E-8 ± 1.49599E-8	-9.52318E-11 ± 1.65388E-11

frequency increases. The magnitudes of A_2 to A_5 indicate the higher-order frequency-dependent effects on the loss tangent. Coefficient B1 introduces a hydration-time-dependent effect with a negative value of B1 (-0.02634), implying a decrease in the loss tangent as hydration time increases. Coefficients B2 to B5 represent higher-order hydration-time-dependent effects, highlighting the intricate relationship between hydration time and the loss tangent for DM10. The model's goodness of fit can be evaluated using the reduced chi-square value (59.03796), the R-square (0.59235), and the adjusted R-square (0.59078) values. These values indicate that the model captures a substantial portion of the variance in the data. However, the relatively high reduced chi-square value indicates some degree of uncertainty or noise in the model.

The dielectric constant values for mix 6 (DM30), which involves a 30 wt% replacement of cement with diatomite, offer intriguing insights into the impact of diatomite content on the material's dielectric behavior, as shown in Fig. 11(a). At 200 MHz, the initial dielectric constant values exhibit significant variation over time. They start at 31.55 F/m, then notably decrease before experiencing a significant increase at around 44.52 F/m. Finally, they stabilize at higher values, ranging from 48.88 F/m to 49.87 F/m. As the frequency escalates to 1000 MHz and beyond, the dielectric constant values display a consistent and gradual decline over time intervals. Commencing at 24.48 F/m and ascending to 48.15 F/m at 240 minutes, followed by a decline to 44.57 F/m at 360 minutes for 1000 MHz and 37.21 F/m for 6500 MHz. This fluctuation highlights the complex interaction between diatomite content and the evolving microstructure, leading to changes in energy storage capacity.[27] At 2000 MHz to 6500 MHz frequencies, the dielectric constant values follow a similar pattern. The values start lower, experience fluctuations, and then gradually stabilize or slightly increase.

The unique behavior observed in mix DM30 can be attributed to the complex interplay between diatomite, pore structure modifications, and ion mobility.[65,66] The initial fluctuations at 200 MHz could be indicative of microstructural adjustments triggered by the addition of diatomite, which then settles into a more stable pattern. Notably, the decreasing trend in dielectric constant values at higher frequencies indicates a reduced ability to store electrical energy. This behavior can be attributed to changes in the material's porosity, conductivity, and ion migration influenced by diatomite content. Compared to mix DM10, mix DM30 demonstrates a higher range of dielectric constant values, reflecting the intensified influence of diatomite at a higher dosage. The fluctuating pattern at lower frequencies is consistent with a dynamic microstructure undergoing hydration-induced changes. In comparison, the stabilization at higher frequencies suggests a balanced electromagnetic response as the material matures.

The loss tangent values of mix DM30 provide crucial insights into its energy dissipation behavior across various frequencies and testing durations, as shown in Fig. 11(b). Notably, the loss tangent values exhibit a dynamic trend marked by fluctuations across frequencies and testing times. At a frequency of 200 MHz, the loss tangent values exhibit some fluctuation, ranging from 0.14 to 1.67 over the 360-minute testing period. This variability suggests that the energy dissipation capability of DM30 at this frequency is inconsistent and may be influenced by factors such as microstructural changes or moisture content.[37,42,58] As the frequency increases to 1000 MHz, the loss tangent values decrease from 0.16 to 0.43. This decreasing trend indicates that DM30 becomes more efficient in dissipating energy at higher frequencies, possibly due to the nature of energy propagation and dissipation mechanisms at play.[18,59] The decreasing trend in loss tangent values continues as the frequency rises to 2000 MHz, where the values range from 0.08 to 0.30. This trend suggests that DM30 exhibits improved energy dissipation behavior as the frequency increases, making it suitable for applications that involve higher frequencies.

Further testing at 3000 MHz reveals a similar pattern, with the loss tangent values ranging from 0.09 to 0.29. This trend highlights the ability of DM30 to dissipate energy at even higher frequencies effectively. The loss tangent values at 4000, 5000, and 6000 MHz also exhibit consistent trends, reflecting a decrease in values as frequency increases. This behavior aligns with the overall trend observed in this testing, showcasing DM30's enhanced energy dissipation capabilities at higher frequencies. At 6500 MHz, the loss tangent values again follow the decreasing trend, ranging from 0.14 to 0.37. This trend underscores DM30's potential for effective energy dissipation even at high frequencies.

Table 14 provides a statistical model that offers a profound understanding of the complex interactions between frequency, hydration time, and the dielectric constant of DM30. The constant term (z0) represents the dielectric constant at the reference frequency and hydration time. The coefficients A_1 to A_5 capture the frequency-dependent effects on the dielectric constant, with the negative value of A_1 (-1.03579×10^{-8}) implying a slight decrease in the dielectric constant with increasing frequency, suggesting possible relaxation

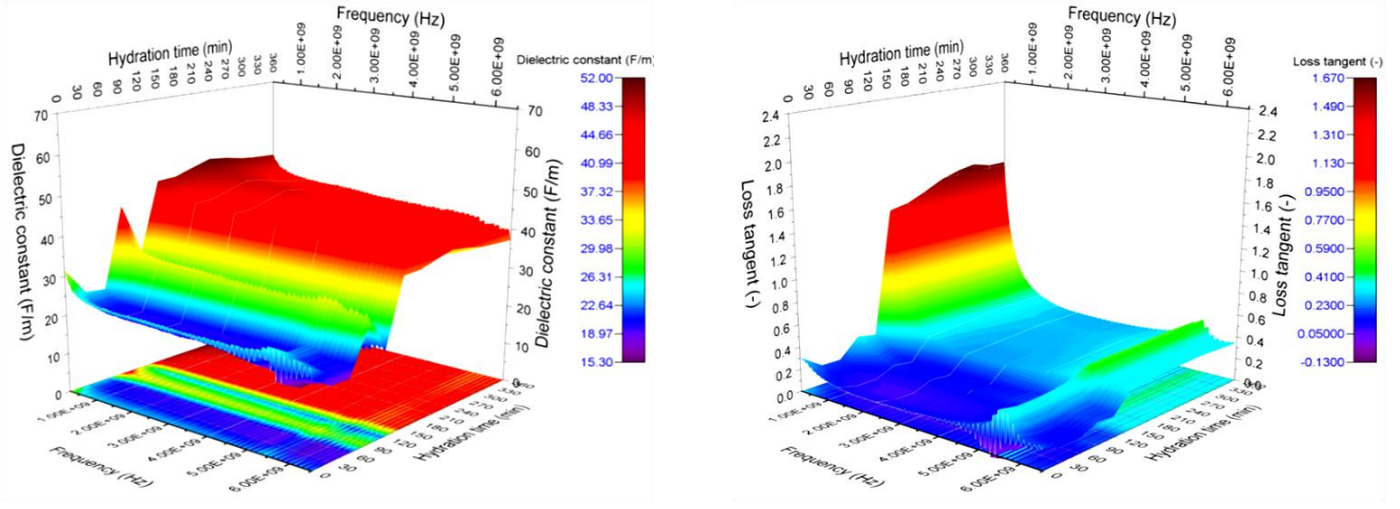

(a) Dielectric constant (ε') (b) Loss tangent ($tan\ \delta$)

Fig. 11 The 3D graph illustrating the simultaneous influence of frequency and hydration time on the dielectric constant and loss tangent of 70 wt% eco-efficient cement-30 wt% diatomite paste.

Table 14. The statistical model for predicting dielectric constant values of 70 wt% eco-efficient cement-30 wt% diatomite paste.

z0	**A_1**	**A_2**	**A_3**	**A_4**	**A_5**
31.1538 ± 0.70044	-1.03579E-8 ± 1.79868E-9	6.27222E-18 ± 1.55969E-18	-1.80459E-27 ± 5.73023E-28	2.39863E-37 ± 9.32929E-38	-1.21886E-47 ± 5.54479E-48
R^2	**B_1**	**B_2**	**B_3**	**B_4**	**B_5**
0.88693	-0.25701 ± 0.01538	0.00481 ± 2.93769E-4	-2.09116E-5 ± 2.15991E-6	3.13148E-8 ± 6.71363E-9	-1.03133E-11 ± 7.4222E-12

phenomena within the material.[18] The coefficients B_1 to B_5 correspond to the effects of hydration time on the dielectric constant, with a negative coefficient for B_1 (-0.25701) indicating that longer hydration times are associated with lower dielectric constants. This trend could arise from changes in the material's microstructure and porosity as it progresses through hydration. The reduced chi-square value (11.89023) corroborates the model's effectiveness, indicating a reasonable fit between the model and the observed data. The relatively high R-square value (0.88737) and adjusted R-square (0.88693) signify that the model explains a significant proportion of the dielectric constant's variance.

The polynomial 2D model developed for DM30's loss tangent provides valuable insights into the electrical behavior of the material, considering both frequency and hydration time, as shown in Table 15. The constant term (z0) represents the loss tangent at a reference frequency and hydration time, with a value of 1.06891, indicating that DM30 exhibits a low loss tangent behavior compared to other mixtures. Coefficients A_1 to A_5 capture frequency-dependent effects, with the negative value of A_1 (-1.66311×10^{-9}) suggesting that the loss tangent decreases with increasing frequency. The magnitudes of A_2 to A_5 indicate the presence of higher-order frequency-dependent effects on the material's loss tangent. Coefficient B1 introduces a hydration-time-dependent effect, with a negative value of B1(-0.00405), implying a decrease in the loss tangent with increasing hydration time. Coefficients B2 to B5 contribute to higher-order hydration-time-dependent effects, highlighting the intricate relationship between hydration time and the loss tangent for DM30. The model's goodness of fit can be evaluated using the reduced chi-square value (0.00836), the R-square (0.76317), and the adjusted R-square (0.76226) values. These values indicate that the model explains a significant portion of the variance in the data, with a relatively low reduced chi-square value indicating a good fit.

3.4 Dielectric properties of eco-efficient cement-silica fume pastes

The dielectric constant values observed in mix SF8 (8 wt% replacement of eco-efficient cement by silica fume) provide

Table 15. The statistical model for predicting loss tangent values of 70 wt% eco-efficient cement-30 wt% diatomite paste.

z0	**A_1**	**A_2**	**A_3**	**A_4**	**A_5**
1.06891 ± 0.01857	-1.66311E-9 ± 4.76856E-11	1.06676E-18 ± 4.13496E-20	-3.20896E-28 ± 1.51917E-29	4.55545E-38 ± 2.47333E-39	-2.44772E-48 ± 1.47001E-49
R^2	**B_1**	**B_2**	**B_3**	**B_4**	**B_5**
0.76226	-0.00405 ± 4.07644E-4	6.94188E-5 ± 7.78824E-6	-3.31765E-7 ± 5.72625E-8	6.37333E-10 ± 1.77988E-10	-4.22663E-13 ± 1.96774E-13

valuable insights into how silica fume influences the dielectric behavior of the eco-efficient cement paste, as shown in Fig. 12(a). At a frequency of 200 MHz, there is an exciting trend in the dielectric constant values over time. They start at 57.59 F/m and progressively increase, reaching 80.74 F/m at 360 minutes. This consistent rise suggests that adding silica fume impacts the material's ability to store electrical energy. The dielectric constant values display a similar pattern when transitioning to higher frequencies, particularly at 1000 and 2000 MHz. The values steadily climb, starting at 53.83 F/m and 50.99 F/m, respectively, reinforcing the enhanced energy storage capabilities introduced by the silica fume. This trend is consistent with the increased ion mobility and electrical conductivity often associated with supplementary cementitious materials like silica fume.[28,31,46,68]

The dielectric constant values at frequencies of 3000 MHz and above also indicate a continuous upward trend. This trend suggests that silica fume enhances the material's overall energy storage capacity across various frequencies. This behavior aligns with the known effects of supplementary materials on the porosity and microstructure of cementitious materials, leading to improved ion movement and energy storage.[1–3,39,69] The increasing trend in dielectric constant values in mix SF8 points toward the potential of silica fume as a beneficial additive for cementitious materials. The improved energy storage characteristics observed across different frequencies indicate the increased electrical conductivity and ion mobility induced by the silica fume, contributing to the overall dielectric behavior of the material.

The loss tangent values of eco-efficient cement paste with an 8 wt% replacement of cement by silica fume (SF8) provide valuable insights into its energy dissipation behavior across different frequencies and testing durations, as shown in Fig. 12(b). These values offer an understanding of how adding silica fume influences the material's ability to dissipate energy, which is essential for various engineering applications. At the lowest frequency of 200 MHz, the loss tangent values for SF8 ranged from 2.78 to 3.62 during the 360-minute testing period. This initial range indicates the material's relatively high energy dissipation capacity at this frequency range. The values exhibit slight fluctuations over time, suggesting a nuanced behavior that may be attributed to material settling and microstructural changes during testing.[28] As the frequency increases to 1000 MHz, the loss tangent values decrease and stabilize, ranging from 0.69 to 0.84. This reduction in the loss tangent indicates that the eco-efficient cement paste with silica fume at higher frequencies demonstrates improved energy dissipation capabilities, potentially due to enhanced interfacial interactions between the cementitious matrix and silica fume particles.[39,46,47,59,68,70]

At 2000 MHz and beyond, the loss tangent values stabilize, ranging from 0.46 to 0.54. This range demonstrates the material's consistent energy dissipation behavior at these higher frequencies, suggesting that adding silica fume contributes to stable energy dissipation characteristics within this frequency range. Interestingly, the loss tangent values at 5000 MHz exhibit a unique behavior, remaining relatively constant at around 0.34. This behavior could be attributed to specific interactions between the silica fume particles and the electromagnetic waves at this frequency range, resulting in consistent energy dissipation behavior.

The statistical model developed for SF8 elucidates the complex interactions between frequency, hydration time, and the material's dielectric constant, as shown in Table 16. The constant term (z0) represents the dielectric constant at the reference frequency and hydration time. The coefficients A_1 to A_5 encode frequency-dependent effects, with the negative value of A_1 (-2.64916×10^{-8}) suggesting that the dielectric constant decreases slightly as frequency increases, implying the presence of relaxation mechanisms. The coefficients B_1 to B_5 correspond to the impact of hydration time on the dielectric constant, with the positive value of B_1 (0.58406) implying that

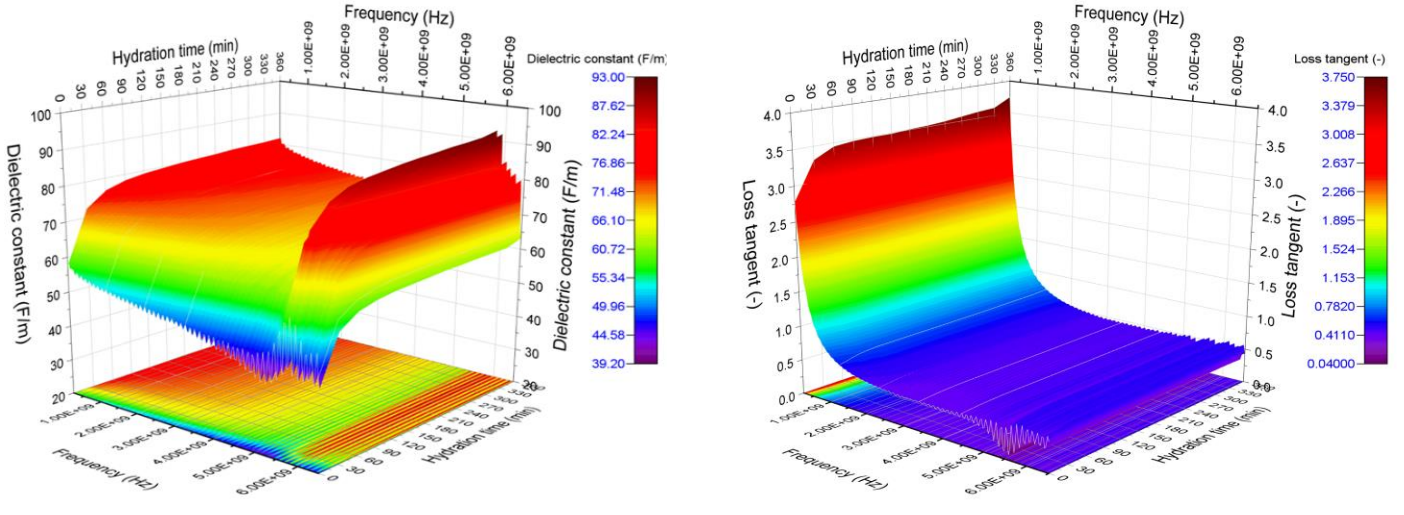

(a) Dielectric constant (ε') (b) *tan* δ– Measuring results

Fig. 12 The 3D graph illustrating the simultaneous influence of frequency and hydration time on the dielectric constant and loss tangent of 92 wt% eco-efficient cement -8 wt% silica fume paste.

Table 16. The statistical model for predicting dielectric constant values of 92 wt% eco-efficient cement -8 wt% silica fume paste.

z0	A_1	A_2	A_3	A_4	A_5
64.69864 ± 0.8327	-2.64916E-8 ± 2.13831E-9	2.24661E-17 ± 1.85419E-18	-8.65862E-27 ± 6.81223E-28	1.43045E-36 ± 1.10909E-37	-8.33959E-47 ± 6.59178E-48
R^2	B_1	B_2	B_3	B_4	B_5
0.74553	0.58406 ± 0.01828	-0.00665 ± 3.49239E-4	3.59029E-5 ± 2.56776E-6	-9.04118E-8 ± 7.98133E-9	8.56447E-11 ± 8.82369E-12

longer hydration times are associated with higher dielectric constants. This trend could arise from changes in the material's microstructure and porosity as it undergoes hydration.[1–3] The reduced chi-square value (16.80451) indicates the model's effectiveness, signifying a reasonable fit between the model and the experimental data. In contrast, the R-square value (0.7465) and adjusted R-square (0.74553) suggest that the model explains a substantial portion of the dielectric constant's variance

The polynomial 2D model for the loss tangent of SF8 provides valuable insights into the material's behavior in terms of loss tangent, considering the effects of frequency and hydration time, as shown in Table 17. The constant term (z0) indicates the loss tangent at a reference frequency and hydration time. With a value of 3.54749, SF8 exhibits a moderate loss tangent behavior compared to other mixtures. The coefficients A_1 to A_5 capture frequency-dependent effects, with the negative value of A_1 (-5.183×10^{-9}) suggesting that the loss tangent decreases as the frequency increases. The small magnitudes of A_2 to A_5 indicate that the frequency-dependent effects are relatively weak in SF8. Coefficients B_1 to B_5 contribute to hydration-time-dependent effects. Its positive value of B_1 (0.00234) implies an increased loss tangent with increasing hydration time. Coefficients B_2 to B_5 introduce higher-order hydration-time-dependent effects, indicating the intricate relationship between hydration time and the loss tangent. The model's goodness of fit can be evaluated using the reduced chi-square value (0.01438), the R-square (0.93079), and the adjusted R-square (0.93052) values. These values suggest that the model fits the data well, explaining a significant portion of the variance.

The dielectric constant values recorded for SF15, involving a 15 wt% replacement of cement by silica fume, offer valuable insights into the influence of silica fume content on the dielectric behavior of eco-efficient cement paste, as shown in Fig. 13(a). At 200 MHz, the dielectric constant values consistently increase over the testing duration, starting at 49.81 F/m and progressively rising to 77.81 F/m at 360 minutes. This remarkable trend underscores the significant enhancement in energy storage capacity at this frequency due to the presence of silica fume. Transitioning to 1000 MHz, a similar pattern unfolds, with dielectric constant values beginning at 46.92 F/m and steadily increasing to 75.39 F/m. This ongoing rise highlights the improved energy storage potential attributed to the incorporation of silica fume.[68,70,71]

The upward trend continues at frequencies of 2000 MHz and beyond. Starting at 45.66 F/m and reaching 73.45 F/m, the values indicate an overall augmentation in energy storage capabilities as the frequency increases, driven by the presence of a higher dosage of silica fume. The observed trends demonstrate the substantial impact of the 15 wt% silica fume replacement on the dielectric behavior of eco-efficient cement paste. The consistent increase in dielectric constant values suggests an evolving electrical behavior tied to the presence of silica fume, which could be attributed to its enhanced pozzolanic activity, increased surface area, and altered pore structure.[7,15] Mix SF15 stands out with its clear and persistent rise in dielectric constant values across all frequencies and over time. This trend illustrates the substantial impact of silica fume on improving the energy storage capacity of eco-efficient cement paste. The results align with the concept that introducing silica fume leads to improved ion mobility, altered porosity, and enhanced energy storage capabilities under the influence of electric fields.[28,31,42,69]

The loss tangent values of eco-efficient cement paste in mix SF15 provide insights into its energy dissipation behavior across different frequencies and testing durations, as shown in Fig. 13(b). At the lowest frequency of 200 MHz, the loss tangent values of SF15 range from 2.98 to 3.51 over the 360-minute testing period. These values indicate relatively high energy dissipation, suggesting that SF15 exhibits significant energy loss at lower frequencies. The small fluctuations in the loss tangent values over time suggest consistent energy dissipation behavior within this frequency range. As the frequency increases to 1000 MHz, the loss tangent values decrease, consistently ranging from 0.70 to 0.79. This reduction in energy dissipation capabilities at higher frequencies signifies SF15's improved efficiency in

Table 17. The statistical model for predicting loss tangent values of 92 wt% eco-efficient cement -8 wt% silica fume paste.

z0	A_1	A_2	A_3	A_4	A_5
3.54749 ± 0.02436	-5.183E-9 ± 6.25425E-11	3.1894E-18 ± 5.42324E-20	-9.10882E-28 ± 1.99248E-29	1.21222E-37 ± 3.24392E-39	-6.0793E-48 ± 1.928E-49
R^2	B_1	B_2	B_3	B_4	B_5
0.93052	0.00234 ± 5.34649E-4	-2.76357E-5 ± 1.02147E-5	1.51117E-7 ± 7.51032E-8	-3.81798E-10 ± 2.33442E-10	3.64238E-13 ± 2.5808E-13

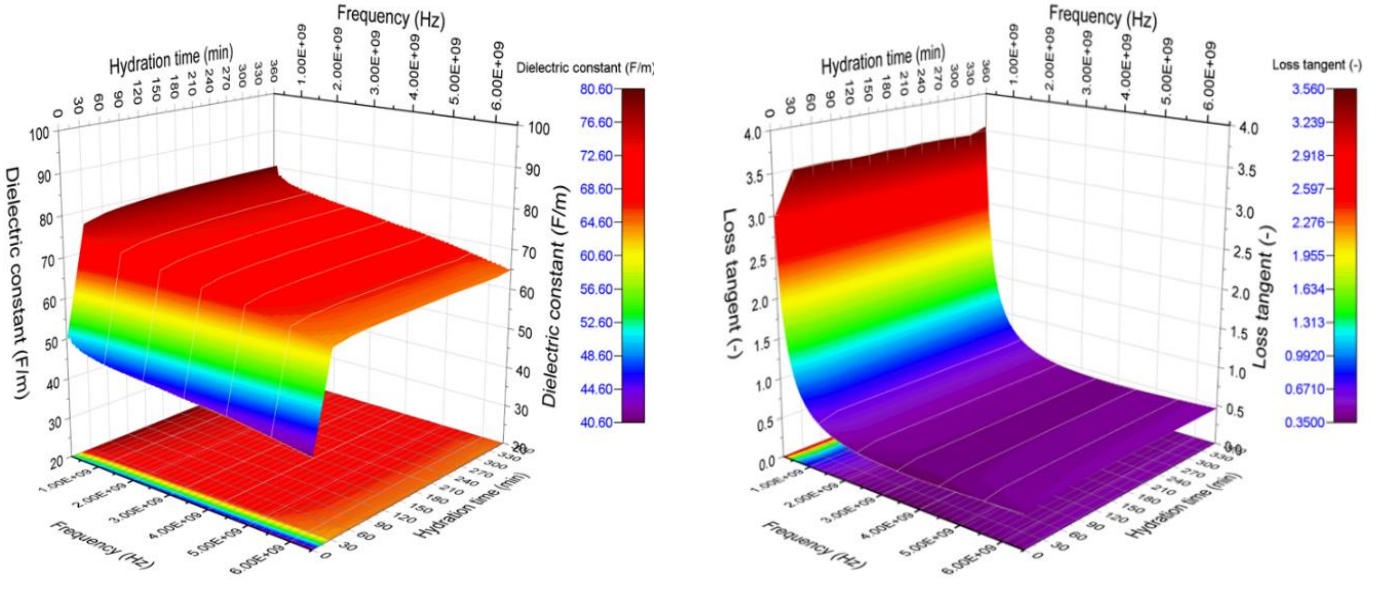

(a) Dielectric constant (ε') (b) Loss tangent ($tan\ \delta$)

Fig. 13 The 3D graph of the simultaneous influence of frequency and hydration time on the dielectric constant and loss tangent of 85 wt% eco-efficient cement -15 wt% silica fume paste.

transmitting electromagnetic signals or minimizing energy loss in these ranges.

Decreasing loss tangent values continue as the frequency rises to 2000 MHz and beyond. The loss tangent values remain stable, oscillating between 0.44 and 0.50. This stability indicates SF15's sustained ability to control energy dissipation even as the frequency increases. The consistent and stable loss tangent values of SF15 across different frequencies and testing durations suggest its suitability for applications that require controlled energy dissipation, particularly in the higher frequency ranges. The decreasing trend of loss tangent with increasing frequency aligns with the expected behavior of materials that minimize energy loss, making SF15 potentially valuable for applications involving electromagnetic wave transmission or signal processing.

The statistical model developed for SF15 unravels the intricate relationships between frequency, hydration time, and the material's dielectric constant, as shown in Table 18. The constant term (z0) signifies the dielectric constant at the reference frequency and hydration time. Coefficients A_1 to A_5 introduce frequency-dependent effects. The negative value of A_1 (-8.19098×10^{-9}) suggests a slight decline in the dielectric constant with increasing frequency, implying the presence of relaxation mechanisms. Coefficients B_1 to B_5 capture the impact of hydration time on the dielectric constant. The coefficient B_1 (0.99679) indicates that higher hydration times increase dielectric constants. This behavior can be attributed to changes in the material's microstructure and porosity during hydration. The reduced chi-square value (2.13162) indicates the model's effectiveness, suggesting a good fit between the model and the experimental data. Furthermore, the high R-square value (0.96494) and adjusted R-square (0.96481) affirm that the model explains a significant portion of the dielectric constant's variability.

The polynomial 2D model for the loss tangent of SF15 provides valuable insights into the material's behavior regarding the loss tangent, considering both frequency and hydration time, as shown in Table 19. The constant term (z0) represents the loss tangent at a reference frequency and hydration time. With a value of 3.53227, SF15 exhibits a moderate loss tangent behavior compared to other mixtures. The coefficients A_1 to A_5 capture the frequency-dependent effects. The negative value of A_1 (-5.3194×10^{-9}) suggests that the loss tangent decreases with increasing frequency. The magnitudes of A_2 to A_5 are relatively small, indicating weak frequency-dependent effects in SF15. Coefficients B1 to B5 contribute to hydration-time-dependent effects. The positive value of B1 (0.00274) implies that the loss tangent tends to increase with longer hydration times. Coefficients B2 to B5 introduce higher-order hydration-time-dependent effects,

Table 18. The statistical model for predicting dielectric constant values of 85 wt% eco-efficient cement -15 wt% silica fume paste.

z0	**A_1**	**A_2**	**A_3**	**A_4**	**A_5**
54.91745 ± 0.29657	-8.19098E-9 ± 7.61576E-10	4.05776E-18 ± 6.60385E-19	-1.14311E-27 ± 2.42623E-28	1.51257E-37 ± 3.95011E-38	-7.74846E-48 ± 2.34771E-48
R^2	**B_1**	**B_2**	**B_3**	**B_4**	**B_5**
0.96481	0.99679 ± 0.00651	-0.01332 ± 1.24384E-4	7.78951E-5 ± 9.14527E-7	-2.05693E-7 ± 2.84261E-9	2.00798E-10 ± 3.14263E-12

Table 19. The statistical model for predicting loss tangent values of 85 wt% eco-efficient cement -15 wt% silica fume paste.

z0	A_1	A_2	A_3	A_4	A_5
3.53227 ± 0.01931	-5.3194E-9 ± 4.95966E-11	3.38862E-18 ± 4.30067E-20	-1.01031E-27 ± 1.58005E-29	1.41145E-37 ± 2.57245E-39	-7.44199E-48 ± 1.52892E-49
R^2	B_1	B_2	B_3	B_4	B_5
0.95185	0.00274 ± 4.23981E-4	-3.76087E-5 ± 8.10036E-6	2.26052E-7 ± 5.95574E-8	-6.13354E-10 ± 1.85121E-10	6.15253E-13 ± 2.04659E-13

revealing the complex interaction between hydration time and the loss tangent. The model's quality of fit can be assessed using the reduced chi-square value (0.00904), the R-square (0.95204), and the adjusted R-square (0.95185) values. These values indicate that the model provides an excellent fit to the data, explaining a significant portion of the variance.

4. Discussion

The dielectric constant is a critical property in cementitious materials, providing valuable insights into their microstructural changes and hydration processes.[7,8,10,15–18,28,72] Analyzing the dielectric constant and loss tangent across eco-efficient cement paste mixtures reveals significant variations in their behavior. Factors such as the type and dosage of pozzolan can influence the behavior of the dielectric constant, leading to diverse trends in response to frequency and hydration time. Polynomial 2D models for each mixture can capture and illustrate these trends. Including pozzolanic materials like fly ash, calcium carbonate, diatomite, and silica fume creates unique interactions with the cement matrix, resulting in diverse dielectric behaviors. The dielectric characteristics of these materials make them well-suited for specific applications in which their dielectric properties play a vital role.

4.1 Time-dependent effects

Time-dependent variations in dielectric properties are crucial for understanding the behavior of cementitious materials, particularly in construction and infrastructure applications. Cement hydration is the process in which cement particles react with water to form a solid matrix, a time-dependent phenomenon. As hydration progresses, the material transforms from a mixture of dry components into a hardened structure with unique electrical characteristics.[2,4,9,28,33] In this discussion, we explore the intricacies of time-dependent variations in dielectric properties and shed light on how these changes impact the performance and durability of cementitious materials.

During the initial stages of cement hydration, which typically occur from the moment water is introduced to the mix to a few hours after that, significant variations in dielectric properties occur.[20,28,73-74] The dissolution of cement compounds, such as tricalcium silicate (C_3S) and dicalcium silicate (C_2S), leads to the formation of calcium silicate hydrates (C-S-H) and calcium hydroxide (CH). At this point, the material exhibits high porosity and a relatively low degree of hydration. These changes primarily result from the initial dissolution of cement particles and the subsequent release of ions into the pore solution.[2,4,8,9]

A prominent observation during this phase is the rapid increase in the dielectric constant. This surge can be attributed to free water in the system. Due to its high dielectric constant, water molecules dominate the electrical response during this period. As cement particles dissolve, they release ions into the pore solution, contributing to ionic polarization and further elevating the dielectric constant.[10,15,16,18,19] Simultaneously, the loss tangent often decreases during the early stages of hydration. This reduction indicates diminishing ionic mobility as the concentration of ions in the pore solution increases, signifying the shift from free water-dominated electrical behavior to a state where ions become more influential.[66,75,78]

As the hydration process advances from a few hours to several days, the dielectric properties continue to evolve, transitioning into intermediate stages. This phase is characterized by the formation of calcium silicate hydrate (C-S-H) gel, a pivotal component of cementitious materials.[3–5] During this transition, the dielectric constant tends to stabilize or even decrease as the initial dominance of free water diminishes. This reduction occurs as free water becomes bound within the porous structure of the C-S-H gel, which has a lower dielectric constant than free water. This transition reflects the changing composition of the material and its increasing solid content.[10,42] Simultaneously, the loss tangent often decreases or stabilizes during these intermediate stages. The reduction in ionic mobility persists as the material solidifies. This phase is characterized by the development of the C-S-H gel and the densification of the material's microstructure.[9,16,79]

A common trend emerged in all the pozzolanic eco-efficient cement paste mixes studied: an increase in the dielectric constant over time.[28,42] This behavior can be attributed to several factors. Firstly, ongoing hydration reactions form products with different dielectric properties than the initial constituents.[1,3] These new products contribute to increased polarization and capacitance within the material, thus influencing the dielectric constant.[7–10,47] Secondly, the development of the pore structure, including capillary pores and interfacial zones, can affect the ease with which charges migrate through the material, thereby influencing its dielectric response.[8,17–18,20,47] Additionally, the formation of bound water in the cementitious matrix and the establishment of a more complex microstructure contribute to changes in polarization mechanisms over time.[10,15–18,20,33] Moreover, loss tangent values also exhibit a time-dependent increase, indicating

higher energy dissipation and enhanced friction between components within the mix. This phenomenon is closely related to the increased internal friction due to the changing microstructure.[28]

4.2 Frequency-dependent effects

Frequency is a crucial parameter that profoundly influences the dielectric response of cementitious materials, as demonstrated in this research. Dielectric properties, particularly the dielectric constant (ε') and loss tangent ($tan\ \delta$), are central to understanding how materials store electrical energy and dissipate it in the form of heat when subjected to an electric field.

At lower frequencies, typically below a few kilohertz, dielectric materials, including cementitious ones, behave as insulators.[63] They exhibit high dielectric constants due to polarization effects stemming from the sluggish reorientation of dipoles within the material in response to the applied electric field. This polarization often involves phenomena such as the alignment of polar molecules.[31,80] However, dielectric materials transform behavior when we shift to higher frequencies, typically in the megahertz and gigahertz range.[16,18,37,81-83] They can no longer keep pace with the rapidly oscillating electric field, resulting in reduced polarization and a decline in the dielectric constant. At these elevated frequencies, materials may display more conductive properties influenced by electrical conductivity and dielectric relaxation factors. One particularly intriguing phenomenon observed in frequency-dependent responses is dielectric relaxation. This process is characterized by a time delay in which dipoles within a material respond to an applied electric field. The rate of this relaxation depends on the frequency of the applied field. Materials exhibit different relaxation times at various frequencies, leading to a complex dielectric response. These relaxation processes are often defined by a relaxation time constant (τ) that quantifies how rapidly dipoles reorient themselves in response to the field.[4,18,26,32,84-85].

In the context of this study, we observed a frequency-dependent trend in the dielectric constant across all types and dosages of pozzolan examined. This trend manifested as a decrease in the dielectric constant as the frequency increased. Such a pattern implies the existence of relaxation mechanisms within the material, which directly relate to the interactions between charge carriers and the dynamic relaxation phenomenon.[4,32] Furthermore, the frequency-dependent behavior of the loss tangent in cementitious materials signifies the interplay between charge carriers and these relaxation mechanisms. At higher frequencies, charge carriers face limitations in responding to alternating fields, resulting in reduced energy dissipation. The intricate interplay between charge migration, relaxation mechanisms, and frequency-dependent behavior contributes to the complex electrical response observed in these materials.[32,62,82]

4.3 Pozzolan-type effect

The influence of the pozzolan type on the dielectric properties of cementitious materials is a crucial aspect of contemporary construction and materials science. Pozzolans, as supplementary cementitious materials (SCMs), have gained substantial attention for their ability to enhance the performance and sustainability of cement-based materials.[40] Fly ash, calcium carbonate, diatomite, and silica fume are pozzolans that impart unique properties, significantly affecting the dielectric behavior of eco-efficient cement pastes and concretes. Each pozzolan type possesses distinctive characteristics, resulting in unique dielectric constant values and loss tangent trends. These differences arise from variations in particle size, reactivity, and surface chemistry.[35,39,42,43,47] Understanding these effects is essential for material optimization.

The dielectric implications associated with different pozzolans:

(i) Fly ash: This commonly used pozzolan is derived from coal combustion in power plants and is known for its fine particle size and spherical morphology. When integrated into cementitious materials, fly ash enhances the dielectric constant. This increase arises from the high silica content of fly ash, which amplifies polarization effects.[28,31,37,47,56-58]

(ii) Calcium carbonate: It is also known as limestone or chalk and is occasionally employed as a pozzolan. It is abundant and cost-effective. Particle size and purity influence the dielectric properties of cement paste with calcium carbonate. Generally, introducing calcium carbonate decreases the dielectric constant.[63,64]

(iii) Diatomite: This natural pozzolan comprises fossilized diatoms and microscopic algae with intricate skeletal structures. Eco-efficient cement pastes containing diatomite exhibit intriguing dielectric behaviors. The porous nature of diatomite can affect the dielectric constant, with modulations driven by factors like diatomite content and particle size.[65,66,86]

(iv) Silica fume: An ultrafine pozzolan composed of highly reactive amorphous silica particles, silica fume is renowned for enhancing the mechanical properties of cementitious materials. Its addition to eco-efficient cement pastes generally leads to an increase in the dielectric constant. This behavior arises from silica fume particles' high surface area and pozzolanic reactivity [39,46,47,62,68,71,87]

Furthermore, the dielectric constant baseline (z0) exhibits substantial variation with the pozzolan type, indicating the intrinsic electrical properties of the pozzolans themselves. These disparities arise from particle characteristics, surface charges, and interactions with the cementitious matrix. Additionally, coefficients A_1 and B_1, representing frequency and time dependence, respectively, reveal the distinct contributions of each pozzolan to relaxation mechanisms, charge redistribution, and ongoing hydration reactions.

4.4 Pozzolan-dosage effect

The influence of pozzolan dosage on dielectric properties is readily discernible through coefficient variations and baseline

values. Higher pozzolan dosages consistently result in elevated dielectric constants and loss tangent values. This trend underscores the heightened polarization effects and increased interfacial interactions arising from a higher concentration of pozzolanic particles.[75] The increase in dielectric constants signifies the prevalence of polarization mechanisms within the system, while the augmented loss tangent values denote enhanced energy dissipation attributed to additional interfaces and relaxation mechanisms.[4,7,10,31,33]

The delicate equilibrium between pozzolan dosage and resultant electrical properties underscores the critical importance of precise material design. The quantity of pozzolan incorporated into cementitious materials, often called dosage or replacement level, plays a pivotal role in determining dielectric properties. The effects of pozzolan dosage can be summarized as follows:

(i) Optimum dosage: Determining the optimal pozzolan dosage is paramount for achieving the desired dielectric properties. An inadequate dosage may fall short of providing the expected enhancements, while an excessive dosage could lead to diminishing returns or adverse effects on other material properties.[35,39]

(ii) Strength and porosity: Higher pozzolan dosages typically enhance the compressive strength and reduce the porosity of cementitious materials. These alterations can influence the dielectric constant and loss tangent.[69,88]

(iii) Pore structure: Pozzolans can refine the pore structure of eco-efficient cement pastes, thereby affecting the connectivity and distribution of water within the material. These changes in pore structure, in turn, impact dielectric properties by altering dielectric relaxation behavior.[41,43,88,89]

(iv) Time-dependent behavior: The influence of pozzolan dosage on dielectric properties may evolve due to the ongoing hydration process. This time-dependent behavior necessitates prolonged investigations to capture the complete spectrum of the impact of pozzolanic reactions.[28]

In a comparative analysis, it becomes evident that the effects of pozzolan type and dosage outweigh the influence of frequency and time, highlighting the predominant role of these factors in shaping dielectric properties. Pozzolans characterized by high reactivity, such as silica fume, exhibit more pronounced variations in dielectric constant values and loss tangent behaviors. Furthermore, augmented dosages amplify the impact of pozzolan type on electrical properties, underscoring the potential for tailored material design based on specific application requirements.

4.5 Analytical modeling of dielectric properties

Analytical modeling of dielectric properties in cementitious materials is a powerful tool for understanding the complex electrical behavior of these materials. By formulating mathematical models and equations, researchers and engineers can predict and optimize dielectric constants and loss tangents under various conditions, thus providing valuable insights for material design and performance evaluation.[26,28,90-92] One notable analytical model is the rational 2D model, which describes the dielectric properties of materials, including cement paste, with different types and dosages of pozzolans. This model considers the real and imaginary components of the dielectric constant and loss tangent, thus providing a comprehensive understanding of how these properties change under different circumstances.[93]

Investigating time-dependent fluctuations in dielectric properties is crucial for understanding the evolution of cementitious materials during the hydration process. The rational 2D model can capture these dynamic changes by considering the contributions of different phases as they occur over time. For example, during the early stages of hydration, there is a sudden increase in the dielectric constant due to the ingress of water into pores and the dissolution of cement compounds. As hydration progresses, the formation of hydration products, such as C-S-H gel, further affects the dielectric properties. The rational 2D model accurately quantifies these temporal transitions.

Frequency-dependent responses in dielectric properties are also significant in modeling. The rational 2D model can predict the changes in the dielectric constant and loss tangent as the frequency varies. At lower frequencies, the dielectric constant increases as water molecules and ions polarize in response to the electric field. As the frequency increases, the dominant factor shifts towards ion mobility and relaxation mechanisms within the material. The rational 2D model effectively stimulates and analyzes these modulations in dielectric behavior across a wide frequency range, mirroring the experimental findings effectively.

The influence of different pozzolan types and dosages on dielectric properties is a crucial focus of this study, and the rational 2D model is a valuable tool in this regard. It incorporates each pozzolan type's specific chemical and physical attributes (fly ash, calcium carbonate, diatomite, and silica fume). It dynamically adjusts the concentration of pozzolan particles in the model to simulate the impact of different dosages. This versatility allows researchers to investigate how introducing these pozzolans affects dielectric behavior and gain insights into the underlying mechanisms.

The strength of the rational 2D model lies in its predictive ability. By calibrating model parameters based on empirical data, researchers can extrapolate the potential trends of dielectric properties under various scenarios. For example, the model can predict the long-term behavior of cementitious materials under specific pozzolan dosages, thus aiding in informed decision-making for material composition optimization. Analytical modeling, particularly when utilizing the rational 2D model, is a valuable tool for optimizing material formulations. It enables the identification of optimal pozzolan dosages to achieve desired dielectric properties, whether for improved durability or reduced energy dissipation. This approach aligns with the principles of sustainable construction by promoting the use of industrial by-products like fly ash and silica fume, fostering innovation and eco-

friendliness in the construction industry.[1,3]

4.6 Challenges and future requirements

Challenges and prospects for the future: Understanding the time-dependent changes in dielectric properties provides valuable insights into the complex processes occurring in cementitious materials during hydration. These subtle variations significantly affect the electrical behavior of the material, ultimately impacting its performance and durability. By thoroughly understanding these dynamic changes, researchers and engineers can make informed decisions regarding mixed designs, quality control protocols, and the long-term performance evaluations of construction materials. These efforts collectively advance the development of sustainable and resilient construction materials.[34,47] The study of frequency-dependent responses in dielectric materials is an area of significant research interest with broad implications in various fields, including electronics and medical diagnostics.[28] The continuous search for materials with precisely tailored electrical properties across a wide range of frequencies drives the advancement of this field. Ongoing research in this area holds the potential to discover new opportunities in technology, communication, and the broader field of materials science. Understanding the influence of pozzolan type and dosage on dielectric properties is highly significant in construction and materials engineering.

(i) Sustainability: Pozzolans play a crucial role in sustainable construction practices by reducing the amount of clinker in cement, which helps to decrease carbon emissions. The selection and amount of pozzolan used in cementitious materials are vital to maximizing sustainability benefits.[1-2,34,59,94-97]

(ii) Performance enhancement: The dielectric behavior of cementitious materials is critical in determining their durability and long-term operational effectiveness. Carefully using pozzolan can improve dielectric properties, benefiting electrical insulation and providing better protection against electrical corrosion.[3,14,59,83,94–98]

(iii) Material design: The choice and amount of pozzolan play a crucial role in the customized design of specialized cementitious materials for specific applications. Eco-efficient cement pastes with high dielectric properties can serve as electrical insulators, whereas those with lower dielectric properties may be preferable in specific structural components.[18,27,31,99-100]

(iv) Quality control: Quality control in the production of cement-based products requires vigilant monitoring of dielectric properties. Deviances from expected dielectric behaviors can act as a warning, indicating problems in material compositions or curing processes.[3,7,10,101,102]

The need for construction materials that are both durable and environmentally friendly is becoming increasingly important. Understanding the electrical behavior of pozzolans in this context is crucial. Analytical modeling of dielectric properties in cementitious materials presents distinct challenges. These challenges include the need for models that accurately represent the complex interaction of microstructural elements and the necessity of empirical data to validate these models. Advanced modeling techniques, such as machine learning, can enhance predictive accuracy and broaden the scope of materials encompassed within these models. These efforts, supported by continuous scientific investigation, offer the potential to uncover innovative paths in the ongoing pursuit of advanced building materials and environmentally friendly infrastructure.

5. Conclusions

This study examined the dielectric constant and loss tangent of various eco-efficient cement paste mixes with different types and dosages of pozzolan. The results demonstrated significant variations in electrical behavior among the samples, providing valuable insights into the electrical properties of cementitious materials and their potential implications for structural performance. Key findings and conclusions include the following:

- The type of pozzolanic material substantially impacted the electrical properties of the eco-efficient cement paste. Mixtures containing fly ash, calcium carbonate, diatomite, and silica fume exhibited distinct variations in behavior. The dosages of pozzolanic materials directly influenced the electrical properties of the cementitious mixes, highlighting the importance of precise material proportions for achieving desired electrical characteristics.
- The quantity of fly ash present significantly affects the dielectric constant and loss tangent of eco-efficient cement paste. Increasing the fly ash content resulted in a decrease in the dielectric constant and an increase in the loss tangent, indicating improved electrical resistivity.
- Eco-efficient cement pastes mixed with different levels of calcium carbonate replacement displayed unique electrical characteristics. The dielectric constant decreased as the dosage of calcium carbonate increased, suggesting a reduction in ionic conduction. The dosage and hydration time affected the loss tangent values, highlighting the intricate relationship between these parameters.
- The addition of diatomite caused distinct electrical reactions in eco-efficient cement paste blends. The dielectric constant values exhibited variations in response to different amounts of diatomite, suggesting changes in the material's polarizability. The loss tangent values of the eco-efficient cement paste showed complex relationships with both frequency and hydration time, indicating various charge accumulation and relaxation mechanisms.
- The electrical properties of the eco-efficient cement paste were significantly influenced by adding silica fume, with the extent of these changes depending on the dosage. The

dielectric constant values showed a non-linear correlation with the dosage of silica fume, indicating an improvement in material compactness. The loss tangent values exhibited diverse frequency and hydration duration patterns, highlighting complex charge-related phenomena.

- Statistical models were developed and found to have high predictive accuracy for each mixture's dielectric constant and loss tangent. These models optimize eco-efficient cement paste formulations to achieve the desired electrical properties.
- Eco-efficient cement pastes with adaptable dielectric properties are versatile and suitable for various applications. High dielectric constant pastes serve as electrical insulators, while lower properties are suitable for structural components. These materials show potential in a wide range of applications, from electromagnetic interference shielding to capacitors, highlighting their potential to drive innovation and impact across various industries.
- The study delved into the fundamental processes, such as charge accumulation and relaxation, that govern the electrical behavior of cementitious materials. This understanding significantly enhances our knowledge of material behavior. The study's primary contribution lies in its ability to tailor the electrical properties of eco-efficient cement paste for specific applications. These include construction, infrastructure, and electronics, where specific electrical characteristics are crucial. The potential impact of this research on these industries is significant, offering new possibilities for the development of eco-efficient materials.

Acknowledgements
This project is funded by National Research Council of Thailand (NRCT) and Phranakhon Rajabhat University (No. N42A660379). We acknowledge the support of Rajamangala University of Technology Phra Nakhon during the project.

Conflict of Interest
There is no conflict of interest.

Supporting Information
Applicable.

References
[1] K. L. Scrivener, V. M. John, E. M. Gartner, Eco-efficient cements: potential economically viable solutions for a low-CO_2 cement-based materials industry, *Cement and Concrete Research*, 2018, **114**, 2-26, doi: 10.1016/j.cemconres.2018.03.015.
[2] K. E. Kurtis, Innovations in cement-based materials: addressing sustainability in structural and infrastructure applications, *MRS Bulletin*, 2015, **40**, 1102-1109, doi: 10.1557/mrs.2015.279.
[3] H. M. Saleh, S. B. Eskander, Innovative cement-based materials for environmental protection and restoration, New Materials in Civil Engineering. Amsterdam: Elsevier, 2020.
[4] C. Tsonos, I. Stavrakas, C. Anastasiadis, A. Kyriazopoulos, A. Kanapitsas, D. Triantis, Probing the microstructure of cement mortars through dielectric parameters' variation, *Journal of Physics and Chemistry of Solids*, 2009, **70**, 576-583, doi: 10.1016/j.jpcs.2008.12.015.
[5] D. Marchon, R. J. Flatt, Mechanisms of cement hydration, Science and Technology of Concrete Admixtures. Amsterdam: Elsevier, 2016.
[6] G. C. Bye, Portland Cement: Composition, Production and Properties, 2nd edition. Thomas Telford Ltd, 1999.
[7] P. Shen, L. Lu, Y. He, F. Wang, S. Hu, Hydration monitoring and strength prediction of cement-based materials based on the dielectric properties, *Construction and Building Materials*, 2016, **126**, 179-189, doi: 10.1016/j.conbuildmat.2016.09.030.
[8] W. J. McCarter, A. B. Afshar, Monitoring the early hydration mechanisms of hydraulic cement, *Journal of Materials Science*, 1988, **23**, 488-496, doi: 10.1007/BF01174674.
[9] A. M. Ley-Hernandez, J. Lapeyre, R. Cook, A. Kumar, D. Feys, Elucidating the effect of water-to-cement ratio on the hydration mechanisms of cement, *ACS Omega*, 2018, **3**, 5092-5105, doi: 10.1021/acsomega.8b00097.
[10] L. Xie, Z. Xia, S. Xue, X. Fu, Detection of setting time during cement hydration using ground penetrating radar, *Journal of Building Engineering*, 2022, **60**, 105166, doi: 10.1016/j.jobe.2022.105166.
[11] K. J. Bois, R. Mirshahi, R. Zoughi, Dielectric mixing models for cement based materials. Thompson DO, Chimenti DE, Review of Progress in Quantitative Nondestructive Evaluation. Boston, MA: Springer, 1997.
[12] I. L. Al-Qadi, R. Mostafa, W. Su, S. M. Riad, Measuring dielectric properties of Portland cement concrete: new methods. Structural Materials Technology, CRC Press, 2020.
[13] D. Xu, L. Qin, S. Huang, X. Cheng, Fabrication and properties of piezoelectric composites designed for process monitoring of cement hydration reaction, *Materials Chemistry and Physics*, 2012, **132**, 44-50, doi: 10.1016/j.matchemphys.2011.10.050.
[14] D. Xu, S. Huang, L. Qin, L. Lu, X. Cheng, Monitoring of cement hydration reaction process based on ultrasonic technique of piezoelectric composite transducer, *Construction and Building Materials*, 2012, **35**, 220-226, doi: 10.1016/j.conbuildmat.2012.02.094.
[15] P. Shen, Z. Liu, Study on the hydration of young concrete based on dielectric property measurement, *Construction and Building Materials*, 2019, **196**, 354-361, doi: 10.1016/j.conbuildmat.2018.11.150.
[16] S. Ait Hamadouche, T. Honorio, T. Bore, F. Benboudjema, F. Daout, E. Vourc'h, Dielectric permittivity of C-S-H, *Cement and Concrete Research*, 2023, **169**, 107178, doi: 10.1016/j.cemconres.2023.107178.
[17] J. Liu, Y. Li, C. Jin, H. Lin, H. Li, Y. Li, Y. Liu, Multi-scale quantitative study on dielectric properties of C–S–H synthesized

by different molar ratio of Ca/Si, *Construction and Building Materials*, 2022, **360**, 129599, doi: 10.1016/j.conbuildmat.2022.129599.
[18] T. T. Dinh, S. Hegler, M. Liebscher, I. Navarro de Sosa, H. Li, D. Plettemeier, W.-G. Drossel, V. Mechtcherine, Dielectric material characterization of concrete in GHz range in dependence on pore volume and water content, *Construction and Building Materials*, 2021, **311**, 125234, doi: 10.1016/j.conbuildmat.2021.125234.
[19] J. Liu, Y. Li, Y. Li, C. Jin, H. Lin, H. Li, Quantitative study on the dielectric properties of tricalcium silicate pastes under different W/C, *Construction and Building Materials*, 2023, **366**, 130245, doi: 10.1016/j.conbuildmat.2022.130245.
[20] T. Honorio, T. Bore, F. Benboudjema, E. Vourc'h, M. Ferhat, Dielectric properties of the pore solution in cement-based materials, *Journal of Molecular Liquids*, 2020, **302**, 112548, doi: 10.1016/j.molliq.2020.112548.
[21] D. Buerchler, B. Elsener, H. Boehni, Electrical resistivity and dielectric properties of hardened cement paste and mortar, *MRS Online Proceedings Library*, 1995, **411**, 407-412, doi: 10.1557/PROC-411-407.
[22] B. Akuthota, R. Zoughi, K. E. Kurtis, Determination of dielectric property profile in cement-based materials using microwave reflection and transmission properties, Proceedings of the 21st IEEE Instrumentation and Measurement Technology Conference. Como, Italy. IEEE, 2004.
[23] G. A. Niklasson, A. Berg, K. Brantervik, B. Hedberg, L. O. Nilsson, Dielectric properties of porous cement mortar: Fractal surface effects, *Solid State Communications*, 1991, **79**, 93-96, doi: 10.1016/0038-1098(91)90486-f.
[24] M. Perez-Pena, D. M. Roy, A. S. Bhalla, L. E. Cross, Dielectric properties of densified hardened cementitious materials, *Cement and Concrete Research*, 1986, **16**, 951-965, doi: 10.1016/0008-8846(86)90019-0.
[25] A.V. Beek, K.V. Breugel, M.A. Hilhorst, Monitoring system for hardening concrete based on dielectric properties. In: R.K. Dhir, M.C. Limbachiya (Eds), Utilizing Ready Mix Concrete and Mortar, Proceedings of the International Conference Held at the University of Dundee, Thomas Telford, UK. 1999, 303-312, doi: 10.1680/urcam.28234.0028
[26] S. O. Nelson, A. W. Kraszewski, Dielectric properties of materials and measurement techniques, *Drying Technology*, 1990, **8**, 1123-1142, doi: 10.1080/07373939008959939.
[27] C. Phrompet, C. Sriwong, C. Ruttanapun, Mechanical, dielectric, thermal and antibacterial properties of reduced graphene oxide (rGO)-nanosized C3AH6 cement nanocomposites for smart cement-based materials, *Composites Part B: Engineering*, 2019, **175**, 107128, doi: 10.1016/j.compositesb.2019.107128.
[28] N. Makul, P. Rattanadecho, D. K. Agrawal, Applications of microwave energy in cement and concrete–A review, *Renewable and Sustainable Energy Reviews*, 2014, **37**, 715-733, doi: 10.1016/j.rser.2014.05.054.
[29] A. Šantić, M. Čalogović, L. Pavić, J. Gladić, Z. Vučić, D. Lovrić, K. Prskalo, B. Janković, Z. Tarle, A. Moguš-Milanković, New insights into the setting processes of glass ionomer cements from analysis of dielectric properties, *Journal of the American Ceramic Society*, 2015, **98**, 3869-3876, doi: 10.1111/jace.13830.
[30] D. A. Triana-Camacho, J. H. Quintero-Orozco, E. Mejía-Ospino, G. Castillo-López, E. García-Macías, Piezoelectric composite cements: towards the development of self-powered and self-diagnostic materials, *Cement and Concrete Composites*, 2023, **139**, 105063, doi: 10.1016/j.cemconcomp.2023.105063.
[31] D. D. L. Chung, X. Xi, A review of cement-based materials as electroceramics, *Ceramics International*, 2023, **49**, 24621-24642, doi: 10.1016/j.ceramint.2023.05.107.
[32] C. Rayssi, S. El.Kossi, J. Dhahri, K. Khirouni, Frequency and temperature-dependence of dielectric permittivity and electric modulus studies of the solid solution $Ca_{0.85}Er_{0.1}Ti_{1-x}Co_{4x/3}O_3$ ($0 \leq x \leq 0.1$), *RSC Advances*, 2018, **8**, 17139-17150, doi: 10.1039/c8ra00794b.
[33] N. Dilissen, J. Vleugels, J. Vermeiren, B. García-Baños, J. R. S. Marín, J. M. Catalá-Civera, Temperature dependency of the dielectric properties of hydrated and ordinary Portland cement and their constituent phases at 2.45GHz up to 1100°C, *Cement and Concrete Research*, 2023, **165**, 107067, doi: 10.1016/j.cemconres.2022.107067.
[34] L. Trigos, J. Gallego, J. I. Escavy, L. Picado-Santos, Dielectric properties versus microwave heating susceptibility of aggregates for self-healing asphalt mixtures, *Construction and Building Materials*, 2021, **293**, 123475, doi: 10.1016/j.conbuildmat.2021.123475.
[35] F. Yousuf, X. Wei, J. Zhou, Monitoring the setting and hardening behaviour of cement paste by electrical resistivity measurement, *Construction and Building Materials*, 2020, **252**, 118941, doi: 10.1016/j.conbuildmat.2020.118941.
[36] C. Zhang, G. P. Panda, Q. Yan, W. Zhang, C. Vipulanandan, G. Song, Monitoring early-age hydration and setting of Portland cement paste by piezoelectric transducers via electromechanical impedance method, *Construction and Building Materials*, 2020, **258**, 120348, doi: 10.1016/j.conbuildmat.2020.120348.
[37] A. B. Malkawi, H. Al-Mattarneh, B. E. Achara, B. S. Mohammed, M. F. Nuruddin, Dielectric properties for characterization of fly ash-based geopolymer binders, *Construction and Building Materials*, 2018, **189**, 19-32, doi: 10.1016/j.conbuildmat.2018.08.180.
[38] M. Jamil, M. K. Hassan, H. M. A. Al-Mattarneh, M. F. M. Zain, Concrete dielectric properties investigation using microwave nondestructive techniques, *Materials and Structures*, 2013, **46**, 77-87, doi: 10.1617/s11527-012-9886-2.
[39] F. Massazza, Pozzolanic cements, *Cement and Concrete Composites*, 1993, **15**, 185-214, doi: 10.1016/0958-9465(93)90023-3.
[40] M. Juenger, J. L. Provis, J. Elsen, W. Matthes, R. D. Hooton, J. Duchesne, L. Courard, H. He, F. Michel, R. Snellings, N. De Belie, Supplementary cementitious materials for concrete: characterization needs, *MRS Online Proceedings Library*, 2012, **1488**, 8-22, doi: 10.1557/opl.2012.1536.
[41] S. Demis, J. G. Tapali, V. G. Papadakis, An investigation of the effectiveness of the utilization of biomass ashes as pozzolanic

materials, *Construction and Building Materials*, 2014, **68**, 291-300, doi: 10.1016/j.conbuildmat.2014.06.071.
[42] W. L. Lai, S. C. Kou, W. F. Tsang, C. S. Poon, Characterization of concrete properties from dielectric properties using ground penetrating radar, *Cement and Concrete Research*, 2009, **39**, 687-695, doi: 10.1016/j.cemconres.2009.05.004.
[43] M. Karim, M. Hossain, M. Khan, M. Zain, M. Jamil, F. Lai, On the utilization of pozzolanic wastes as an alternative resource of cement, *Materials*, 2014, **7**, 7809-7827, doi: 10.3390/ma7127809.
[44] O. A. Mohamed, A. A. Farghali, A. K. Eessaa, A. M. El-Shamy, Cost-effective and green additives of pozzolanic material derived from the waste of alum sludge for successful replacement of Portland cement, *Scientific Reports*, 2022, **12**, 20974, doi: 10.1038/s41598-022-25246-7.
[45] S. Jumrat, B. Chatveera, P. Rattanadecho, Dielectric properties and temperature profile of fly ash-based geopolymer mortar, *International Communications in Heat and Mass Transfer*, 2011, **38**, 242-248, doi: 10.1016/j.icheatmasstransfer.2010.11.020.
[46] Y. Zhong, P. Wang, B. Zhang, Y. Wang, T. Liu, X. Li, Y. Niu, Research on detection method of concrete compressive strength based on dielectric properties, *Journal of Building Engineering*, 2023, **76**, 107090, doi: 10.1016/j.jobe.2023.107090.
[47] Y. Li, Y. Liu, C. Jin, J. Mu, J. Liu, Research on mechanical and electromagnetic shielding properties of cement paste with different contents of fly ash and slag, *NDT & E International*, 2023, **133**, 102736, doi: 10.1016/j.ndteint.2022.102736.
[48] R. He, T. Nantung, J. Olek, N. Lu, Use of dielectric constant for determination of water-to-cement ratio (W/C) in plastic concrete: part 2: comparison determined W/C values by ground penetrating radar (GPR) and microwave oven drying measurements, *ES Materials & Manufacturing*, 2023, **22**, 874, doi: 10.30919/esmm5f874.
[49] S. Huang, X. Meng, G. Zhao, Z. Liu, Development and engineering application of cement-based full length anchoring material, *ES Materials & Manufacturing*, 2023, **23**, 1051, doi: 10.30919/esmm1051.
[50] ASTM International, "ASTM C1157", Standard Performance Specification for Hydraulic Cement, American Society for Testing and Materials, USA, 2019.
[51] ASTM International, "ASTM C618", Standard Specification for Coal Fly Ash and Raw or Calcined Natural Pozzolan for Use in Concrete, American Society for Testing and Materials, USA.
[52] ASTM International, "ASTM C1240", Standard Specification for Silica Fume Used in Cementitious Mixtures, American Society for Testing and Materials, USA, 2020.
[53] ASTM International, "ASTM C494", Standard Specification for Chemical Admixtures for Concrete, American Society for Testing and Materials, USA, 2017.
[54] "Data sheet," E5080A ENA Vector Network Analyzer, Keysight Technologies, 2023.
[55] C. Phrompet, C. Sriwong, S. Maensiri, P. Chindaprasirt, C. Ruttanapun, Optical and dielectric properties of nano-sized tricalcium aluminate hexahydrate (C3AH6) cement, *Construction and Building Materials*, 2018, **179**, 57-65, doi: 10.1016/j.conbuildmat.2018.05.180.
[56] B. Canımkurbey, Investigation dielectric and morphological properties of fly ash collected from thermal power plant, *Asia-Pacific Journal of Chemical Engineering*, 2020, **15**, e2437, doi: 10.1002/apj.2437.
[57] M. N. Soutsos, J. H. Bungey, S. G. Millard, M. R. Shaw, A. Patterson, Dielectric properties of concrete and their influence on radar testing, *NDT & E International*, 2001, **34**, 419-425, doi: 10.1016/s0963-8695(01)00009-3.
[58] W. Chen, P. Shen, Z. Shui, Determination of water content in fresh concrete mix based on relative dielectric constant measurement, *Construction and Building Materials*, 2012, **34**, 306-312, doi: 10.1016/j.conbuildmat.2012.02.073.
[59] S. Baranek, V. Cerny, R. Drochytka, L. Meszarosova, J. Melichar, Electrically conductive composite materials with incorporated waste and secondary raw materials, *Scientific Reports*, 2023, **13**, 9023, doi: 10.1038/s41598-023-36287-x.
[60] S. C. Raghavendra, R. L. Raibagkar, A. B. Kulkarni, Dielectric properties of fly ash, *Bulletin of Materials Science*, 2002, **25**, 37-39, doi: 10.1007/BF02704592.
[61] S. Hanjitsuwan, P. Chindaprasirt, K. Pimraksa, Electrical conductivity and dielectric property of fly ash geopolymer pastes, *International Journal of Minerals, Metallurgy, and Materials*, 2011, **18**, 94-99, doi: 10.1007/s12613-011-0406-0.
[62] A. Ashery, A. E. H. Gaballah, E. M. Ahmed, Tuned high dielectric constant, low dielectric loss tangent with positive and negative values for PPy/MWCNTs/TiO_2/Al_2O_3/n-Si, *Journal of Experimental Nanoscience*, 2021, **16**, 309-343, doi: 10.1080/17458080.2021.1973667.
[63] A. Saeed, S. O. Adewuyi, H. A. M. Ahmed, S. R. Alharbi, S. E. Al Garni, F. Abolaban, Electrical and dielectric properties of the natural calcite and quartz, *Silicon*, 2022, **14**, 5265-5276, doi: 10.1007/s12633-021-01318-7.
[64] S. Kobe, G. Dražić, A. C. Cefalas, E. Sarantopoulou, J. Stražišar, Nucleation and crystallization of $CaCO_3$ in applied magnetic fields, *Crystal Engineering*, 2002, **5**, 243-253, doi: 10.1016/s1463-0184(02)00035-7.
[65] G. You, J. Bi, Y. Chen, C. Yin, C. Wang, Effect of diatomite additive on the mechanical and dielectric properties of porous SiO_2-Si_3N_4 composite ceramics, *Journal of Wuhan University of Technology-Mater. Sci. Ed.*, 2016, **31**, 528-532, doi: 10.1007/s11595-016-1404-x.
[66] Z. Yuan, Z. Wang, Z. Guo, Y. Wang, J. Wang, W.-B. Liu, M. Derradji, J. Qiu, Diatomite-filled epoxy resin composites: Curing behavior, dielectric, and thermal properties, *Polymer Composites*, 2022, **43**, 422-429, doi: 10.1002/pc.26386.
[67] C. J. F. Böttcher, O. C. van Belle, P. Bordewijk, A. Rip, D. D. Yue, Theory of electric polarization, *Journal of the Electrochemical Society*, 1974, **121**, 211C, doi: 10.1149/1.2402382.
[68] S. A. A. El-Enein, M. F. Kotkata, G. B. Hanna, M. Saad, M. M. A. El Razek, Electrical conductivity of concrete containing silica fume, *Cement and Concrete Research*, 1995, **25**, 1615-1620, doi: 10.1016/0008-8846(95)00156-5.

[69] Y. Zhong, P. Wang, B. Zhang, C. Cao, X. Du, D. Duan, Y. Ni, Y. Wang, Composite dielectric model for cement concrete considering water saturation, *Journal of Materials in Civil Engineering*, 2023, **35**, doi: 10.1061/jmcee7.mteng-15174.
[70] R. M. Khattab, H. H. Abo-Almaged, H. E. H. Sadek, Effects of some extracted oxides on silica fume waste for mullite preparation: physical, mechanical, optical, magnetic, and dielectric properties, *Materials Chemistry and Physics*, 2022, **281**, 125880, doi: 10.1016/j.matchemphys.2022.125880.
[71] S. Wen, D. D. L. Chung, Effect of admixtures on the dielectric constant of cement paste, *Cement and Concrete Research*, 2001, **31**, 673-677, doi: 10.1016/s0008-8846(01)00475-6.
[72] M. Meng, F. Wang, Theoretical analyses and experimental research on a cement concrete dielectric model, *Journal of Materials in Civil Engineering*, 2013, **25**, 1959-1963, doi: 10.1061/(asce)mt.1943-5533.0000755.
[73] P. R. Camp, S. Bilotta, Dielectric properties of Portland cement paste as a function of time since mixing, *Journal of Applied Physics*, 1989, **66**, 6007-6013, doi: 10.1063/1.343577.
[74] S. Cerveny, S. Arrese-Igor, J. S. Dolado, J. J. Gaitero, A. Alegría, J. Colmenero, Effect of hydration on the dielectric properties of C-S-H gel, *The Journal of Chemical Physics*, 2011, **134**, 034509, doi: 10.1063/1.3521481.
[75] N. Makul, Dielectric permittivity of various cement-based materials during the first 24 hours hydration, *Open Journal of Inorganic Non-Metallic Materials*, 2013, **3**, 53-57, doi: 10.4236/ojinm.2013.34009.
[76] R. Rianyoi, R. Potong, N. Jaitanong, R. Yimnirun, A. Chaipanich, Dielectric, ferroelectric and piezoelectric properties of 0-3 Barium titanate–Portland cement composites, *Applied Physics A*, 2011, **104**, 661-666, doi: 10.1007/s00339-011-6307-2.
[77] A. Berg, G. A. Niklasson, K. Brantervik, B. Hedberg, L. O. Nilsson, Dielectric properties of cement mortar as a function of water content, *Journal of Applied Physics*, 1992, **71**, 5897-5903, doi: 10.1063/1.350488.
[78] N. Makul, P. Keangin, P. Rattanadecho, B. Chatveera, D. K. Agrawal, Microwave-assisted heating of cementitious materials: relative dielectric properties, mechanical property, and experimental and numerical heat transfer characteristics, *International Communications in Heat and Mass Transfer*, 2010, **37**, 1096-1105, doi: 10.1016/j.icheatmasstransfer.2010.06.029.
[79] B. J. Christensen, T. Coverdale, R. A. Olson, S. J. Ford, E. J. Garboczi, H. M. Jennings, T. O. Mason, Impedance spectroscopy of hydrating cement-based materials: measurement, interpretation, and application, *Journal of the American Ceramic Society*, 1994, **77**, 2789-2804, doi: 10.1111/j.1151-2916.1994.tb04507.x.
[80] M. Cabeza, P. Merino, A. Miranda, X. R. Nóvoa, I. Sanchez, Impedance spectroscopy study of hardened Portland cement paste, *Cement and Concrete Research*, 2002, **32**, 881-891, doi: 10.1016/s0008-8846(02)00720-2.
[81] R. H. Haddad, I. L. Al-Qadi, Characterization of Portland cement concrete using electromagnetic waves over the microwave frequencies, *Cement and Concrete Research*, 1998, **28**, 1379-1391, doi: 10.1016/s0008-8846(98)00076-3.
[82] M. Keddam, H. Takenouti, X. R. Nóvoa, C. Andrade, C. Alonso, Impedance measurements on cement paste, *Cement and Concrete Research*, 1997, **27**, 1191-1201, doi: 10.1016/s0008-8846(97)00117-8.
[83] R. He, N. L. Lu, Unveiling the dielectric property change of concrete during hardening process by ground penetrating radar with the antenna frequency of 1.6GHz and 2.6GHz, *Cement and Concrete Composites*, 2023, **144**, 105279, doi: 10.1016/j.cemconcomp.2023.105279.
[84] I. L. Al-Qadi, O. A. Hazim, W. Su, S. M. Riad, Dielectric properties of Portland cement concrete at low radio frequencies, *Journal of Materials in Civil Engineering*, 1995, **7**, 192-198, doi: 10.1061/(asce)0899-1561(1995)7: 3(192).
[85] X. Zhang, X. Z. Ding, C. K. Ong, B. T. G. Tan, J. Yang, Dielectric and electrical properties of ordinary Portland cement and slag cement in the early hydration period, *Journal of Materials Science*, 1996, **31**, 1345-1352, doi: 10.1007/BF00353116.
[86] T. Bore, P. N. Mishra, N. Wagner, M. Schwing, T. Honorio, A. Revil, A. Scheuermann, Coupled hydraulic, mechanical and dielectric investigations on Kaolin, *Engineering Geology*, 2021, **294**, 106352, doi: 10.1016/j.enggeo.2021.106352.
[87] A. Chaipanich, Dielectric and piezoelectric properties of PZT–silica fume cement composites, *Current Applied Physics*, 2007, **7**, 532-536, doi: 10.1016/j.cap.2006.10.016.
[88] V. Sata, C. Jaturapitakkul, K. Kiattikomol, Influence of pozzolan from various by-product materials on mechanical properties of high-strength concrete, *Construction and Building Materials*, 2007, **21**, 1589-1598, doi: 10.1016/j.conbuildmat.2005.09.011.
[89] F. Xing, B. Dong, Z. Li, The study of pore structure and its influence on material properties of cement-based piezoelectric ceramic composites, *Construction and Building Materials*, 2009, **23**, 1374-1377, doi: 10.1016/j.conbuildmat.2008.07.018.
[90] M. Meng, F. Wang, Theoretical analyses and experimental research on a cement concrete dielectric model, *Journal of Materials in Civil Engineering*, 2013, **25**, 1959-1963, doi: 10.1061/(asce)mt.1943-5533.0000755.
[91] R. T. Coverdale, B. J. Christensen, T. O. Mason, H. M. Jennings, E. J. Garboczi, Interpretation of the impedance spectroscopy of cement paste via computer modelling, *Journal of Materials Science*, 1994, **29**, 4984-4992, doi: 10.1007/BF01151088.
[92] M. Meng, Z. Chen, F. Wang, Comprehensive dielectric model of cement concrete including frequency and temperature, *Advances in Cement Research*, 2023, **35**, 167-179, doi: 10.1680/jadcr.21.00196.
[93] Y. Li, Y.F. Zhang, J. Deng, W.H. Dong, J.T. Sun, J. Pan. S. Du, Rational design of heteroanionic two-dimensional materials with emerging topological, magnetic, and dielectric properties, *The Journal of Physical Chemistry Letters*, 2022, **13**, 3594-3601, doi: 10.1021/acs.jpclett.2c00620.

[94] O. Büyüköztürk, T.-Y. Yu, J. A. Ortega, A methodology for determining complex permittivity of construction materials based on transmission-only coherent, wide-bandwidth free-space measurements, *Cement and Concrete Composites*, 2006, **28**, 349-359, doi: 10.1016/j.cemconcomp.2006.02.004.
[95] H. H. Pan, D.-H. Lin, R.-H. Yang, High piezoelectric and dielectric properties of 0–3 PZT/cement composites by temperature treatment, *Cement and Concrete Composites*, 2016, **72**, 1-8, doi: 10.1016/j.cemconcomp.2016.05.025.
[96] S. Soldatov, M. Umminger, A. Heinzel, G. Link, B. Lepers, J. Jelonnek, Dielectric characterization of concrete at high temperatures, *Cement and Concrete Composites*, 2016, **73**, 54-61, doi: 10.1016/j.cemconcomp.2016.01.006.
[97] Y. Shen, Q. Li, S. Xu, Microwave absorption properties of cementitious composites containing carbonyl iron powder (CIP) and fly ash: formation and effect of CIP core–shell structure, *Cement and Concrete Composites*, 2022, **131**, 104559, doi: 10.1016/j.cemconcomp.2022.104559.
[98] R. Wang, F. He, C. Shi, D. Zhang, C. Chen, L. Dai, AC impedance spectroscopy of cement - based materials: measurement and interpretation, *Cement and Concrete Composites*, 2022, **131**, 104591, doi: 10.1016/j.cemconcomp.2022.104591.
[99] P. Xie, Z. Shi, M. Feng, K. Sun, Y. Liu, K. Yan, C. Liu, T. A. A. Moussa, M. Huang, S. Meng, G. Liang, H. Hou, R. Fan, Z. Guo, Recent advances in radio-frequency negative dielectric metamaterials by designing heterogeneous composites, *Advanced Composites and Hybrid Materials*, 2022, **5**, 679-695, doi: 10.1007/s42114-022-00479-2.
[100] K. Chung, L. Yuan, S. Ji, L. Sun, C. Qu, C. Zhang, Dielectric characterization of Chinese standard concrete for compressive strength evaluation, *Applied Sciences*, 2017, **7**, 177, doi: 10.3390/app7020177.
[101] H. Al-Mattarneh, Electromagnetic quality control of steel fiber concrete, *Construction and Building Materials*, 2014, **73**, 350-356, doi: 10.1016/j.conbuildmat.2014.09.101.
[102] S. Wen, D. D. L. Chung, Cement-based controlled electrical resistivity materials, *Journal of Electronic Materials*, 2001, **30**, 1448-1451, doi: 10.1007/s11664-001-0200-2.